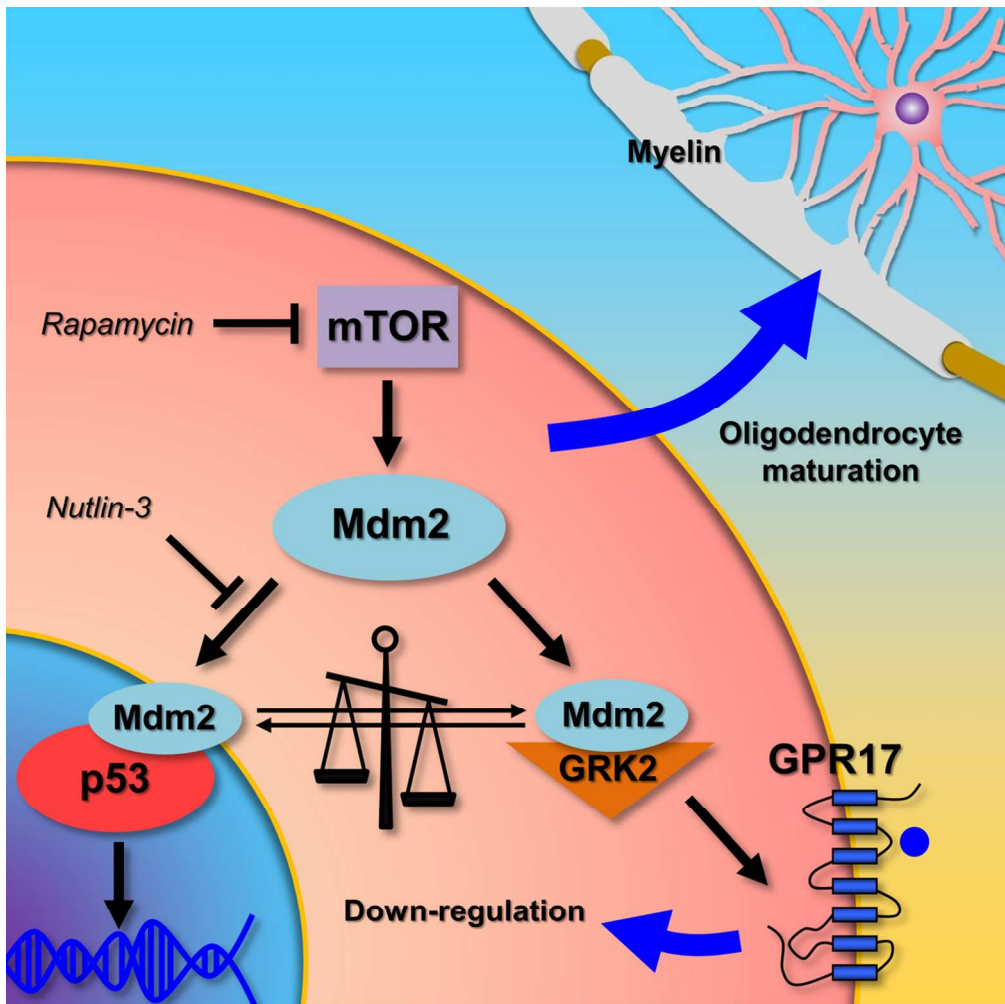




**The ubiquitin ligase Mdm2 controls oligodendrocyte maturation by intertwining mTOR with G protein-coupled receptor kinase 2 in the regulation of GPR17 receptor desensitization**

Journal:	GLIA
Manuscript ID:	GLIA-00101-2015.R1
Wiley - Manuscript type:	Original Research Article
Date Submitted by the Author:	n/a
Complete List of Authors:	Fumagalli, Marta; Università degli Studi di Milano, Dep of Pharmacological and Biomolecular Sciences Bonfanti, Elisabetta; Università degli Studi di Milano, Dep of Pharmacological and Biomolecular Sciences Daniele, Simona; University of Pisa, Dep. of Pharmacy Zappelli, Elisa; University of Pisa, Dep. of Pharmacy Lecca, Davide; Università degli Studi di Milano, Dep of Pharmacological and Biomolecular Sciences Martini, Claudia; University of Pisa, Dep. of Pharmacy Trincavelli, Maria; University of Pisa, Dep. of Pharmacy Abbracchio, Maria; Università degli Studi di Milano, Dep of Pharmacological and Biomolecular Sciences
Key Words:	GPR17 receptor, oligodendrocyte precursor cells, myelination, rapamycin, Nutlin-3

SCHOLARONE™  
Manuscripts



59x59mm (600 x 600 DPI)

**The ubiquitin ligase Mdm2 controls oligodendrocyte maturation by intertwining mTOR  
with G protein-coupled receptor kinase 2 in the regulation of GPR17 receptor  
desensitization**

Marta Fumagalli<sup>a,\*</sup>, Elisabetta Bonfanti<sup>a,\*</sup>, Simona Daniele<sup>b</sup>, Elisa Zappelli<sup>b</sup>, Davide Lecca<sup>a</sup>,  
Claudia Martini<sup>b</sup>, Maria L. Trincavelli<sup>b</sup>, Maria P. Abbracchio<sup>a</sup>

\*These authors equally contributed to the present study

<sup>a</sup>Department of Pharmacological and Biomolecular Sciences, Università degli Studi di  
Milano, 20133 Milan, Italy.

<sup>b</sup>Department of Pharmacy, University of Pisa, 56126 Pisa, Italy.

**Running title:** Mdm2 controls myelination regulating GPR17

**Number of words:**

Abstract:	151
Introduction:	461
Materials and Methods:	<del>1,523</del> 1,893
Results:	<del>1,605</del> 2,016
Discussion:	<del>609</del> 711
Acknowledgements:	63
References:	<del>964</del> 1003
Figure Legends:	<del>1,317</del> 1,747
Number of Figures	<del>5</del> 6 (+ 5 Supplementary Figures)

TOTAL WORD COUNT (including title page) : ~~6890~~ 8055

**Corresponding Author**

Prof. Maria P. Abbracchio

Department of Pharmacological and Biomolecular Sciences, University of Milan, via Balzaretti 9, 20133 Milan, Italy. Tel: +390250318304; Fax: +390250318284;

E-mail: mariapia.abbracchio@unimi.it

**Main points**

- Untimely upregulation of GPR17 impairs oligodendrocyte maturation and myelination
- Mdm2 regulates GPR17 responses at the cell membrane by intertwining mTOR with GRK2
- Unprecedented role for Mdm2 ubiquitin ligase in oligodendrogenesis and myelination

**Keywords:** GPR17 receptor; oligodendrocyte precursor cells; myelination; rapamycin; Nutlin-3

**Abstract**

During oligodendrocyte precursor cell (OPC) differentiation, defective control of the membrane receptor GPR17 has been suggested to block cell maturation and impair remyelination under de-myelinating conditions.

After the immature oligodendrocyte stage, to enable cells to complete maturation, GPR17 is physiologically down-regulated via phosphorylation/desensitization by G protein-coupled Receptor Kinases (GRKs); conversely, GRKs are regulated by the “mammalian target of rapamycin” mTOR. However, how GRKs and mTOR are connected to each other in modulating GPR17 function and oligodendrogenesis has remained elusive.

Here we show, for the first time, a role for Murine double minute 2 (Mdm2), a ligase previously involved in ubiquitination/degradation of the onco-suppressor p53 protein. In maturing OPCs, both rapamycin and Nutlin-3, a small molecule inhibitor of Mdm2-p53 interactions, increased GRK2 sequestration by Mdm2, leading to impaired GPR17 down-regulation and OPC maturation block. Thus, Mdm2 intertwines mTOR with GRK2 in regulating GPR17 and oligodendrogenesis and represents a novel actor in myelination.

## Introduction

Remyelination after central nervous system (CNS) insults is needed to re-establish nerve conduction and prevent axonal loss. Spontaneous remyelination based on recruitment and proliferation of oligodendrocyte precursor cells (OPCs) is defective in diseases such as multiple sclerosis, mainly due to an OPC differentiation block (Franklin and Ffrench-Constant 2008; Kuhlmann et al., 2008). Identifying the mechanisms involved in defective OPC differentiation is important for developing new remyelinating strategies.

The P2Y-like GPR17 receptor responding to uracil-nucleotides and cysteinyl-leukotrienes (cysLTs), two families of mediators involved in CNS repair (Ciana et al., 2006), is a key regulator of OPC maturation (Chen et al., 2009; Coppi et al., 2013; Lecca et al., 2008). GPR17 is expressed by a subpopulation of early OPCs and it is needed to start differentiation; however, GPR17 is turned down before cells reach maturation (Fumagalli et al., 2011). GPR17 responses are regulated by its endogenous ligands; by binding to the receptor, ligands first induce OPCs to undergo differentiation and then switch GPR17 off, inducing its desensitization/down-regulation and cytoplasmic internalization. These latter events involve specific isoforms of G-protein-coupled receptor kinases (GRKs), either GRK2 or GRK5, depending on the class of ligand bound to the receptor (Daniele et al., 2014). Alterations of GPR17 activation and physiological silencing at specific OPC differentiation phases may lead to myelination defects and be even at the basis of demyelinating diseases.

In various *in vivo* neurodegenerative models characterized by myelin loss (stroke, trauma, demyelination and experimental autoimmune encephalomyelitis), GPR17 was abnormally up-regulated in OPCs around lesion sites (Boda et al., 2011; Chen et al., 2009; Lecca et al., 2008). Accordingly, we recently reported that decreased GRKs levels resulting in defective GPR17 desensitization markedly reduce OPC maturation (Daniele et al., 2014). Of interest, altered GRKs expression/activity has been implicated in human inflammatory and demyelinating diseases (Gurevich et al., 2012; Vroon et al., 2005).

GRKs alterations may, in turn, depend on mTOR (the “mammalian target of rapamycin”), a serine/threonine protein-kinase inhibited by the immunosuppressive agent rapamycin (RAPA). mTOR is central to cell growth, differentiation and survival and has been implicated in oligodendrocyte (OL) development and myelination (Tyler et al., 2009). Interestingly, a recent proteomic analysis highlighted increased levels of GPR17 in RAPA-treated OPCs, suggesting this receptor as a putative target for mTOR (Tyler et al., 2011). Despite this initial evidence, the relationships between mTOR, GRKs, GPR17, its interacting proteins and OL maturation have remained elusive.

Here, we demonstrate that, in rat primary OPCs, inhibition of mTOR by RAPA reduces GRK2 levels and prevents GPR17 down-regulation/desensitization, strongly inhibiting OPC maturation. We also prove, for the first time, that Mdm2 (Murine double minute-2), a ligase previously involved in the ubiquitination/degradation of the onco-suppressive p53 protein and in tumor progression (Ashcroft and Vousden 1999) specifically controls OPC maturation by intertwining mTOR with GRK2.

## **Materials and Methods**

### **Oligodendrocyte precursor cell cultures**

Primary OPCs were isolated from mixed glial cultures prepared from postnatal day 2 Sprague–Dawley rat cortex by shaking cells on an orbital shaker at 200 rpm, as previously described (Fumagalli et al., 2011). OPCs were then collected and separated from microglia by incubation for 1h on an uncoated Petri dish. Purified OPCs were seeded onto poly-D,L-ornithine-coated glass coverlips or plates (50 µg/ml, Sigma-Aldrich, Milan, Italy) to a specific density according to the planned experiments (see below), in Neurobasal (Life Technologies, Monza, Italy) with 2% B27 (Life Technologies), 2 mM L-glutamine (EuroClone), 10 ng/ml human platelet-derived growth factor BB (Sigma-Aldrich), and 10

ng/ml human basic fibroblast growth factor (Space Import Export, Milan, Italy), to promote proliferation. After 2 day, cells were switched to a Neurobasal medium lacking growth factors to allow differentiation. In some experiments triiodothyronine T3 (Sigma Aldrich) was also added to a final concentration of 10 ng/ml.

### ***In vitro* pharmacological treatments**

According to the planned experiments, cells were plated in 13 mm glass coverslip or in 60 mm diameter petri dish (20,000 cells/coverslip or 100,000 cells/dish) maintained for 2 days in Neurobasal supplemented with B27 and proliferative factors (PDGF-BB and bFGF) and then, after one day in differentiating medium, cells were treated with either rapamycin (15 nM) (Sigma-Aldrich) or with Nutlin-3 (NUT, 1  $\mu$ M) (Sigma Aldrich). Cells were fixed for immunocytochemistry (ICC) or lysed for WB analysis at day 4 or 6 (see also figure legends for details).

### **Generation of pGPR17-EGFP-N1 plasmid and OPC transfection**

The coding sequence of the human GPR17 receptor was subcloned from a previously generated pcDNA3.1 vector (Life Technologies), using specific primers containing the restriction cassette for XhoI and BamHI (fw: 5'-gtttttctcgagatgaatggcctgaagtggc; rv: 5'-ggtggatccgacagctctgacttggcactca). The product was then inserted upstream to the EGFP sequence in a pEGFP-N1 expression vector (Clontech). For GPR17 over-expression in OPCs, cells were seeded on 13 mm poly-D,L-ornithine-coated coverslips ( $2 \times 10^4$  cells/well) in Neurobasal supplemented with B27 and proliferative factors (PDGF-BB and bFGF). Differentiation was then, induced by removing proliferative factors and at day 4, cells were transfected with the fluorescent plasmid pGPR17-EGFP, in parallel to the corresponding fluorescent empty vector, using the transfection reagent NeuroFECT<sup>TM</sup> (Genlantis, San

Diego, CA, USA) according to manufacturer's protocol. After transfection, cells were maintained in differentiating medium supplemented with T3 for additional 48-72 hours and fixed for ICC.

### **OPCs electroporation with a GRK2 plasmid**

GRK2 overexpression was obtained by electroporating OPCs with the Amaxa Rat Oligodendrocyte Nucleofection Kit (Lonza, Milan, Italy) according to the manufacture' instructions. In detail, OPCs were electroporated with 1 µg either of GRK2 plasmid (Origene) or the corresponding empty vector (OriGene, Maryland, USA) with the O-017 program. After electroporation, cells were rapidly seeded on 13 mm poly-D,L-ornithine-coated coverslips ( $5 \times 10^4$  cells/well) in Neurobasal supplemented with B27 and proliferative factors (PDGF-BB and bFGF) and maintained in this medium. In parallel, electroporated OPCs were also seeded on 60 mm poly-D,L-ornithine-coated dish in order to check transfection efficiency by western-blot analysis. After 30 hours, electroporated OPCs were subjected to the cAMP assay (see below)

### **Immunocytochemistry**

Both primary OPCs and OPC-DRG co-cultures were fixed at room temperature with 4% paraformaldehyde (Sigma-Aldrich) in 0.1 M PBS (Euroclone) containing 0.12 M sucrose (Sigma-Aldrich). Labelling was performed incubating cells overnight at 4°C with the following primary antibodies in Goat Serum Dilution Buffer (GSDB; 450 mM NaCl, 20 mM sodium phosphate buffer, pH 7.4, 15% goat serum, 0.3% Triton X-100): rat anti-MBP (1:200; Millipore, Milan, Italy), rabbit anti-GPR17 (1:100; Cayman, Michigan, USA), mouse anti-SMI 31 and mouse anti SMI 32 (1:500; Cell Signaling, Beverly, MA, USA). Cells were then incubated for 1h at RT with the secondary goat anti-rat, goat anti-rabbit or goat anti-mouse

antibody conjugated to Alexa Fluor 555 or Alexa Fluor 488 (1:600 in GSDB; Molecular Probes, Life Technologies). Nuclei were labelled Hoechst-33258 (1:10,000, Molecular Probes, Life Technologies). Coverslips were finally mounted with a fluorescent mounting medium (Dako, Milan, Italy) and analysed under a fluorescence or confocal microscope (LSM510 META, Zeiss). For cell count, 10 or 20 fields were acquired at 20X magnification (at least 3 coverslips for each experimental condition) under an inverted fluorescence microscope (200M; Zeiss) connected to a PC computer equipped with the Axiovision software (Zeiss). Images were collected and cells scored and counted using the ImageJ software.

### **Subcellular localization of Mdm2**

Primary OPCs (stage 3) were treated with medium alone (CTRL) or 15 nM RAPA for 30 min. At the end of treatments, cells were collected and suspended in 5 mM Tris-EDTA (pH 7.4) and nuclear cell fractions were isolated by centrifugation at 1000 x g for 15 min at 4°C. Mdm2 levels were detected in both cytoplasmic and nuclear fractions by immunoblotting using an anti-Mdm2 antibody (Santa Cruz Biotechnology, sc-812; 1:100). GAPDH (Sigma Aldrich, G9545, 1:5000) and hystone H3 (Santa Cruz Biotechnology, sc-8654; 1:100) were analysed from the same samples as loading controls for the cytosolic and nuclear fraction, respectively.

### **Western blot analysis**

Cell lysates were prepared and analysed by WB as previously described (Coppi et al., 2013). Briefly, cells were lysed in lysis buffer (20 mM Tris pH 7.2, 0.5% deoxycholate, 1% Triton, 0.1% SDS, 150 mM NaCl, 1 mM EDTA and 1% proteases inhibitors, Sigma-Aldrich) and, then, approximately 25-30 µg aliquots from each protein sample were loaded on 12%

sodium-dodecylsulphate polyacrylamide gels (for MBP and CNPase) or on 8.5% sodium-dodecylsulphate polyacrylamide gels (for GPR17, NG2, GRK2 and GRK5), and blotted onto nitrocellulose membranes (MBP and CNPase) or PVDF membranes (GPR17, GRK2, GRK5 and NG2) (Bio-Rad Laboratories, Segrate, Milan, Italy). Membranes were saturated with 10% non-fat dry milk in Tris-buffered saline (TBS; 1 mM Tris-HCl, 15 mM NaCl, pH 8) for 1 h at room temperature and incubated overnight at 4°C with the following primary antibodies diluted in 5% non-fat dry milk in TBS: rabbit anti-GPR17 (1:1000, home-made antibody), rat anti-MBP (1:500), rabbit anti-CNPase (1:250; Santa Cruz Biotechnology, Santa Cruz, CA, USA), rabbit anti-GRK2 (sc-562, 1:200; Santa Cruz Biotechnology) and rabbit anti-GRK5 (sc-565, 1:200; Santa Cruz Biotechnology), rabbit anti-phospho mTOR (Ser2448) (1:500; Cell Signaling, Danvers, MA, USA), mouse anti-mTOR (1:1000; Cell Signaling). The following day, membranes were washed in TBS-T (TBS plus 0.1% Tween20® Sigma Aldrich), incubated for 1 h with goat anti-rabbit or goat anti-mouse or goat anti-rat secondary antibodies conjugated to horseradish peroxidase (1:4000, 1:2000 and 1:2000 in 5% non-fat dry milk in TBS respectively; Sigma-Aldrich). Detection of proteins was performed by enhanced chemiluminescence (ECL, Thermo Scientific, Rodano, Milan, Italy) and autoradiography. Non-specific reactions were evaluated in the presence of the secondary antibodies alone. Densitometric analysis of the protein bands was performed with ImageJ software. Band intensities were measured as integrated density volumes (IDV) and expressed as % of control lane values for comparisons between treatment groups.  $\alpha$ -Tubulin (1:1500; Sigma Aldrich) or  $\alpha$ -actin (1:5000; Sigma Aldrich) expression was analysed from the same sample as an internal control and it was used for data normalization.

### **Measurement of cyclic AMP levels**

For OPCs, cells were plated in 24 well-plates and after 6 days in culture in differentiation medium without T3, functional responsiveness of GPR17 was assessed as described, (Daniele et al., 2014; Fumagalli et al., 2011) using 500 nM UDP-glucose or 5 nM LTD<sub>4</sub>, as stimuli. For desensitisation experiments, OPCs were pre-treated with UDP-glucose (5 µM) or LTD<sub>4</sub> (50 nM) for different times (5-120 min), in the absence (control cells) or in the presence of 15 nM rapamycin or 10 µM Nutlin-3. Then, cells were washed with 400 µl of saline and incubated at 37°C for 15 min with 0.4 ml of non-complete Neurobasal in the presence of the phosphodiesterase inhibitor, Ro20-1724 (20 µM) and stimulated with agonists (500 nM UDP-glucose or 5 nM LTD<sub>4</sub>), in the presence of 10 µM Forskolin (FK). Intracellular cAMP levels were measured using a competitive protein binding method, as previously reported (Daniele et al., 2014).

#### **ELISA assay for the detection of GPR17-GRK or Mdm2-GRK immunocomplexes**

OPCs were treated with medium alone (basal), or UDP-glucose (5µM) or with LTD<sub>4</sub> (50 nM), respectively for 30 min. In some experiments, cells were pre-incubated for 15 min with 15 nM rapamycin or 10 µM Nutlin-3. Then, cells were washed twice in ice-cold phosphate-buffered saline, collected by centrifugation, and resuspended in Lysis buffer (20 mM Tris HCl, 137 mM NaCl, 10% glycerol, 1% NONIDET40, 2 mM EDTA, pH 8), containing 1% of the Protease inhibitor Cocktail (Sigma Aldrich, Milan, Italy). Optimal composition of lysis buffer, as well as reaction conditions, were determined in preliminary experiments. Levels of GPR17-GRK or Mdm2-GRK immunocomplexes in OPC lysates, obtained as above described, were quantified using a validated ELISA method (Zappelli et al., 2014). 96-wells were pre-coated with a mouse full-length anti-Mdm2 antibody (sc-965, Santa Cruz Biotechnology, 1:50 in 0.05% Poly-L-Ornithine) or with an anti-N terminus GPR17 antibody (sc-74792, Santa Cruz Biotechnology, 1:50 in 0.05% Poly-L-Ornithine) overnight at room

temperature. After three washes of 5 minutes with 100  $\mu$ l of PBS/Tween 0.1%, cell lysates (50  $\mu$ g in a final volume of 100  $\mu$ l) were transferred to the pre-coated wells for 120 min with a plastic cover or film and kept under constant agitation. Three quick washes were performed with PBS/Tween 0.1% to remove unbound protein, and each well was incubated for 15 min with 1% bovine serum albumin (BSA, Sigma) to block non-specific sites. Then, wells were incubated for 120 min at room temperature with the specific primary antibodies: anti-GRK2 (Santa Cruz Biotechnology, sc-562; 1:400); anti-GRK5 (Santa Cruz Biotechnology, sc-565; 1:400). Wells were washed and incubated for 1 h with a secondary HRP-conjugate antibody (diluted in 5% milk), and washed again. The TMB substrate kit (Thermo Fisher Scientific) allowed a colorimetric quantification of the complex of GRKs with GPR17 or Mdm2. Blanks were obtained processing cell lysates in the absence of the primary antibodies. To avoid cross interactions between the different antibodies, the chosen primary antibody was always from a different species with respect to the antibody used for well pre-coating. Absorbance's values at 450 nm were measured, background subtracted and bar graphs were generated using Graph Pad Prism 4 software (GraphPad Software Inc., San Diego, CA), from which the percentage of association between the two analysed proteins, compared to basal value, were derived.

### **In vivo rapamycin injections.**

C57BL6/J mice were injected daily with either vehicle or rapamycin intraperitoneally at 10 mg/kg body weight (rapamycin was diluted in the vehicle solution from a stock of 20 mg/mL in 100% ethanol immediately before the injection to a final concentration of 0.8 mg/mL PBS, 5% polyethylene glycol-1000, 5% Tween 80, and 4% ethanol) starting at postnatal day (P) 16. On P21, mice were sacrificed, brains were extracted and rapidly frozen at  $-80^{\circ}\text{C}$ . Membrane protein extracts were obtained by tissue homogenization in lysis buffer (20 mM Tris pH 7.2, 0.5% deoxycholate, 1% Triton, 0.1% SDS, 150 mM NaCl, 1 mM EDTA and 1%

proteases inhibitors, Sigma-Aldrich). The homogenate was centrifuged at 1000g for 10 min at 4°C in order to eliminate nuclei. The protein concentration was estimated using the Bio-Rad Protein Assay (Bio-Rad Laboratories s.r.l., Segrate, Italy). Western blot analysis was performed as described below.

### **Statistical analysis**

All results were expressed as mean  $\pm$  S.E. Statistical analysis was done with non-linear multipurpose curve-fitting Graph-Pad Prism program (Graph-Pad). The statistical test used was chosen according to the type of experiment performed and was indicated in the legend of the figure. Three degrees of significance were considered:  $P < 0.05$  (\*),  $P < 0.01$  (\*\*),  $P < 0.001$  (\*\*\*)).

### **Results**

#### **Involvement of mTOR in GPR17 regulation during OPC differentiation**

Cultured OPCs are known to undergo different subsequent stages of differentiation (stages 1-5) when maintained for up to 6 days in vitro (DIV6) when they reach terminal maturation (stage 5 in Figure 1A). Initial data from a proteomic analysis had shown that RAPA increases GPR17 levels in parallel to a reduction of OPC maturation, highlighting GPR17 as a potential target for mTOR and suggesting that receptor silencing is required for OPC terminal maturation (Ceruti et al., 2011; Fumagalli et al., 2011; Lecca et al., 2008). To get more insights in mTOR regulation of GPR17 and on its effects on OPC maturation, as a first step, we performed a detailed immunocytochemical and western blot (WB) analysis of GPR17 in OPCs treated with RAPA from DIV1 and analysed at either DIV4 (Supplementary Figure S1A) or DIV6 (Figure 1B). At DIV6 (stage 5), RAPA markedly reduced the number of terminal MBP<sup>+</sup> OLs and concomitantly increased the number of GPR17<sup>+</sup> cells (Figure 1B).

No changes in total cell number were detected (CTRL:  $527.4 \pm 73.64$ ; RAPA:  $412.6 \pm 55.59$ , Hoechst 33258 staining). WB analysis confirmed a significant GPR17 enhancement in parallel with reduced mature myelin proteins (CNPase and MBP) (Figure 1C). As shown in Supplementary Figure S1A, in RAPA-treated cells, an increase (+38.7%) of GPR17 compared to CTRL was already detected at DIV4 (stage 4), together with reductions of CNPase and MBP. Conversely, RAPA had no effect on GPR17 at DIV3 (data not shown). To confirm that the effects of RAPA on OPC maturation indeed result in impairments of myelination, RAPA-treated cultures also showed a reduction of MBP<sup>+</sup> segments extending along neurofilament (NF)-positive axons in neuronal/OPC co-cultures (Supplementary Figure S1B). To univocally endorse that GPR17 down-regulation is needed for OPC terminal maturation, we then transfected OPCs with a fluorescence reporter plasmid for GPR17 over-expression (GPR17-EGFP). After 3 days, the majority of control OPCs incorporating the empty plasmid underwent maturation, as demonstrated by CNPase expression and large cytoplasmic areas with many branched processes (Figure 1D). Conversely, most OPCs incorporating the vector for GPR17 over-expression kept an immature morphology and showed reduced expression of both CNPase (Figure 1D) and MBP (data not shown). Thus, interference with GPR17 down-regulation resulting in permanently elevated GPR17 levels markedly impairs OPC differentiation.

### **GRK2 plays a key role in mTOR regulation of GPR17 function and OL maturation**

In other cells, mTOR regulates the expression/function of membrane GPCRs by modulating GRKs (Cobelens et al., 2007). We previously showed that, in OPCs, GRKs are involved in GPR17 desensitization/internalization induced by prolonged exposure to its agonists, and that, depending on the type of ligand (either LTD<sub>4</sub> or UDP-glucose), different GRKs (namely, GRK2 or GRK5) are preferentially recruited to regulate GPR17 functional

response (Daniele et al., 2014).

To establish a functional relationship between mTOR and GRK in OPCs, we analysed the expression profile of these GRK isoforms at DIV4 and DIV6 in control and RAPA-treated cells. RAPA significantly decreased GRK2 levels (Figure 2A), whereas no changes in GRK5 were observed (Supplementary Figure S3A). Then, based on previous data showing that GPR17 associates to GRK2 to a higher extent after LTD<sub>4</sub> compared to UDP-glucose (Daniele et al., 2014) (see also Figure 2B), we measured GPR17-GRK2 association in OPCs in absence or presence of RAPA, and after either LTD<sub>4</sub> or UDP-glucose exposure. Consistent with data in Figure 2A, association of GPR17 to GRK2 was significantly decreased by RAPA, particularly when LTD<sub>4</sub> was used to activate GPR17 (Figure 2B). GPR17 is coupled to Gi and its activation by agonists consequently results in marked inhibition of intracellular levels of cAMP (Fumagalli et al., 2011). Accordingly, in OPCs, LTD<sub>4</sub> potently reduces the increases of cAMP levels induced by the cyclase activator FK (Figure 2C). This Gi mediated effect was progressively lost in cells exposed to the agonist for prolonged time periods, suggesting receptor desensitization (white columns in Figure 2C). RAPA markedly prevented LTD<sub>4</sub> induced receptor desensitization despite an initial challenge with this agonist (black columns in Figure 2C), likely due to a decrease in GRK2 levels. In contrast, UDP-glucose, which activates the GRK5-dependent pathway (Daniele et al., 2014) still induced GPR17 desensitization with kinetics similar to control OPCs (Supplementary Figure S3B). **These results** suggest that mTOR regulates GRK2 which, in turn, mediates LTD<sub>4</sub>-induced GPR17 desensitization. **To further confirm this hypothesis and unequivocally relate RAPA-induced decrease in GRK2 levels with loss of GPR17 desensitization, we performed “rescue experiments” by over-expressing GRK2 in OPCs. Electroporation of cells with a GRK2 plasmid indeed resulted in a marked increase of GRK2 protein levels compared to the corresponding empty vector, as shown by western blot analysis (Fig. 2D). To make sure that**

electroporation had no effects on GPR17 desensitization kinetics, we analyzed LTD<sub>4</sub>-mediated loss of GPR17 function in cells electroporated with the corresponding empty vector. In a similar way to standard controls (Fig. 2C), pre-exposure of electroporated OPCs to LTD<sub>4</sub> gradually desensitized GPR17, and, as expected, this effect was prevented by inhibiting mTOR with rapamycin (Supplementary Figure S2). On the contrary, in OPCs electroporated with the GRK2 plasmid, RAPA was no longer able to prevent LTD<sub>4</sub>-induced GPR17 desensitization (black columns compared to white columns in Fig. 2D). Globally, these results confirm that: (i) GRK2 is very important for LTD<sub>4</sub>-induced GPR17 desensitization; (ii) mTOR normally controls GRK2 activation and GPR17 desensitization; (iii) inhibition of mTOR by RAPA results in prevention of GPR17 desensitization, but this effect is surmounted by GRK2 overexpression; (iv) GRK2 is downstream of mTOR in the pathway of GPR17 desensitization.

### **The ubiquitin ligase Mdm2 mediates the interaction between GRK2 and mTOR**

To gain insights into mTOR-mediated mechanisms governing GRK2 levels/activity in OPCs, we analysed the involvement of the ubiquitin ligase Mdm2. This ligase normally acts as a negative regulator of the onco-suppressor p53 protein, but has also been reported to regulate membrane GPCRs by promoting the degradation of GRK2 in cells other than OPC (Freedman et al., 1999; Salcedo et al., 2006; Thut et al., 1997). On this basis, we quantified Mdm2-association to either GRK2 or GRK5 after mTOR inhibition. RAPA significantly enhanced Mdm2 association to GRK2 with no changes in Mdm2-GRK5 complexes, confirming that, in OPCs, Mdm2 is selective for GRK2 (Figure 3A and Supplementary Figure S5). These data are consistent with decreased GRK2 (Figure 2A) and unaltered GRK5 levels in RAPA-treated OPC lysates (Supplementary Figure S3A). To more directly establish a functional link between Mdm2 and GRK2, we took advantage of Nutlin-3, a small-

molecule inhibitor of Mdm2-p53 interactions (Arva et al., 2008), thus making Mdm2 more available for association to GRK2. Nutlin-3 (NUT) markedly enhanced Mdm2-GRK2 association, with negligible effects on the formation of Mdm2-GRK5 complexes (Figure 3B and Supplementary Figure S5). Sequestration of GRK2 by Mdm2 indeed resulted in a marked reduction of GRK2 levels (Figure 3C), suggesting that Mdm2 drives the ubiquitination/degradation of this kinase. A parallel increase of GPR17 together with decreased CNPase levels was also detected after Nutlin-3 (Figure 3D). In line with these data, Nutlin-3 markedly reduced the association of GRK2 to GPR17 after OPC exposure to GPR17 agonists, with a more marked effect after LTD<sub>4</sub> (Figure 3E). Globally, these data suggest that, in OPCs, disruption of Mdm2-p53 interaction favours the association of Mdm2 to GRK2 and its subsequent degradation, thus impairing GRK2 interaction with GPR17 (Figure 3E).

### **mTOR regulates the equilibrium between Mdm2-p53 and Mdm2-GRK2 complexes**

The above data suggest that mTOR signaling would shift the equilibrium from Mdm2-p53 association to Mdm2-GRK2 association, thereby allowing GRK2 to mediate GPR17 desensitization and OPC maturation. To substantiate this hypothesis, we directly assessed the association of Mdm2 to p53 upon RAPA treatment. As shown in Fig. S4, pre-treatment of OPCs with either RAPA or Nutlin-3 for 30 min reduced the association between Mdm2 and p53. Since in other cells (e.g MCF-7 cells) mTOR dependent phosphorylation of Mdm2 stimulates its translocation from the cytoplasm to the nucleus (Mayo et al., 2001; Feng et al., 2004; Salcedo et al., 2006), where it then associates to p53, we reasoned that mTOR inhibition by RAPA could result in reduced levels of nuclear Mdm2 and in elevated expression of cytosolic Mdm2, which in turn can bind to and ubiquitinate GRK2, thus promoting its degradation. To test this hypothesis, Mdm2 protein levels were quantified in the cytosolic and nuclear compartments of OPCs upon treatment with RAPA. Western-blot

analysis (Fig. 3C) showed that RAPA enhanced Mdm2 cytosolic levels while reducing its nuclear concentrations, thus promoting its association to GRK2 with obvious consequences on GPR17 desensitization.

### **Sequestration of GRK2 by Mdm2 prevents GPR17 desensitization and OL maturation**

We then reasoned that Nutlin-3 might also profoundly influence agonist-induced GPR17 desensitization and OPC terminal maturation. Hence, we exposed OPCs to LTD<sub>4</sub> for 5-120 min, a condition normally resulting in a time-dependent loss of GPR17 activity (Figure 2C), in absence or presence of Nutlin-3. As expected, in control treated cells (CTRL), prolonged exposure to LTD<sub>4</sub> resulted in progressive GPR17 desensitization (white columns in Figure 4A). In Nutlin-3-treated cells, GPR17 response to LTD<sub>4</sub> was fully preserved, confirming that under these conditions GRK2 is no longer available for GPR17 desensitization (black columns in Figure 4A). Conversely, in line with the inability of Mdm2 to associate to GRK5 (Figure 3B), UDP-glucose induced a similar time-dependent loss of GPR17 response in both the absence (CTRL) and presence of Nutlin-3 (white and black columns in Figure 4B). We conclude that dissociation of Mdm2-p53 complexes by Nutlin-3 enhances Mdm2-mediated GRK2 degradation, with consequent decreases of GRK2 levels and block of LTD<sub>4</sub>-induced GPR17 desensitization.

To establish whether these effects also correlate with OPC differentiation, cells were first exposed to Nutlin-3 and then treated with LTD<sub>4</sub> to promote OPC maturation. As expected, LTD<sub>4</sub> increased the number of mature MBP-positive cells (Figure 4C). In the presence of Nutlin-3, LTD<sub>4</sub>-induced OPC maturation was reduced (Figure 4C) in line with the block of GPR17 desensitization under these settings (Figure 4A). We also observed a small, but statistically significant, decrease of OPC maturation when Nutlin-3 was applied to cells in the absence of LTD<sub>4</sub> (Figure 4C), to suggest a modulation of the effects induced by

endogenous GPR17 agonists. These data confirm that: (i) increased Mdm2 association to GRK2 reduces the ability of this kinase to desensitize GPR17, and that (ii) the GRK2-GPR17 interaction is required to complete OPC maturation.

Overall, results show that the Mdm2 ligase intertwines mTOR with GRK2 in regulating the GPR17 receptor and OPC maturation, thus unveiling a totally unexpected role for Mdm2 in oligodendrogenesis and myelination (Figure 6).

### **Postnatal *in vivo* treatment with RAPA increases GPR17 levels and reduces both GRK2 and myelin proteins**

In rodents, myelination occurs in early postnatal life (Hamano et al., 1996) and is completed by post-natal day (P) 21. After birth, GPR17 expression is progressively increased to reach maximal peaks at P14 (Boda et al., 2011), after which it is progressively decreased reaching lower stable levels typical of adult life. Consistent with GPR17 anticipating myelination (Chen et al., 2009), massive myelin production followed the peak of GPR17<sup>+</sup> cell density (P7–P14) and occurred concomitantly with the decrease in GPR17<sup>+</sup> cell number (Boda et al., 2011). If the relationships between mTOR, GRK2 and GPR17 detected in cultured OPCs are physiologically relevant, an early *in vivo* postnatal inhibition of mTOR should affect the normal maturation pattern of myelin proteins and also impact on cerebral GPR17 levels. We thus treated mice with either vehicle or RAPA (10 mg/Kg) (Guardiola-Diaz et al., 2012) daily from P16 to P20 (Supplementary Figure S3A), a time window during which GPR17 starts to be down-regulated (Boda et al., 2011). As expected from literature data (Caccamo et al., 2010), RAPA-injected mice displayed a marked reduction of mTOR phosphorylation on Ser2448, to confirm that *in vivo* RAPA-treatment successfully inhibited mTOR activity (Figure 5). Under these conditions, **a statistically significant increase in GPR17 levels was found in parallel to** a reduction of both GRK2 and mature myelin proteins

like CNPase and MBP ~~was found in parallel to increased GPR17 levels~~ (Supplementary Figure 5B). These data fully confirm *in vivo* the relationships between mTOR, GRK2, GPR17 and myelination, suggesting that mTOR regulates postnatal myelination by fine-tuning GPR17 levels and that GPR17 phosphorylation/desensitization by GRK2 is crucially involved in physiological myelination.

## Discussion

Here we show, for the first time, a role of the ubiquitin ligase Mdm2 in oligodendrogenesis and myelination. Specifically, we demonstrate that Mdm2 intertwines the mammalian target of RAPA, mTOR, and the receptor kinase GRK2 in regulating the desensitization/inactivation of the GPR17 receptor, a key actor in OPC maturation to myelinating phenotypes.

Our previous studies highlighted GPR17 as an indispensable player in initiating OPC differentiation but also suggested down-regulation of the receptor is needed to complete cells' maturation. **Our previous studies also demonstrated that GPR17 down-regulation occurs via agonist-induced receptor internalization, leading to a very marked degradation of the agonist-receptor complex in lysosomes and only partial re-recycling of GPR17 to the plasma membrane. The amount of internalized degraded receptor increased as a function of time of agonist exposure, suggesting that receptor re-routing to the membrane may be rather limited after long exposure times and/or at high agonist concentrations (Fratangeli et al., 2013).**

Here, we first unequivocally confirmed that (Chen et al., 2009; Daniele et al., 2014) in cultured OPCs, forced GPR17 expression throughout their entire differentiation cycle impairs cells' maturation. Accordingly, mice aberrantly over-expressing GPR17 under the control of the promoter of CNPase, a relatively late stage marker, displayed myelin dysfunctions,

tremors and precocious death (Chen et al., 2009). Moreover, in various neurodegeneration animal models, OPCs over-expressing GPR17 accumulate at lesion sites (Boda et al., 2011; Chen et al., 2009; Lecca et al., 2008).

We then showed that RAPA-induced mTOR inhibition resulting in aberrant GPR17 up-regulation and reduced OPC differentiation is mediated by GRK2. Indeed, in late OPCs, a reduction of GRK2 expression/activity by RAPA impaired both GPR17 desensitization and OPC maturation (Daniele et al., 2014), suggesting that loss of this kinase (that normally phosphorylates and down-regulates membrane receptors) may be responsible for the persistent GPR17 up-regulation (Daniele et al., 2014). To support the relevance of these findings to an *in vivo* situation, postnatal treatment of mice with RAPA induced a cortical reduction of myelin-related proteins MBP and CNPase, confirming that mTOR signalling is required during myelination active phases (Narayanan et al., 2009). These effects were associated to an *in vivo* increase of GPR17 levels and a reduction of GRK2, suggesting a failure of GPR17 down-regulation, likely due to loss of mTOR control on GRK2. **Of course, since mTOR is such a central signaling hub affecting simultaneously many different pathways, we cannot exclude that, especially in vivo, RAPA is also inducing other effects.**

The crosstalk between mTOR and GRKs (Cobelens et al., 2007; Salcedo et al., 2006) in OPCs has never been investigated before. To address this issue, we focused on Mdm2, an ubiquitin ligase known for controlling p53 degradation and cancer malignancy (Ashcroft and Vousden 1999). In various types of human cancers, Mdm2 serves as an ubiquitin ligase that promotes p53 degradation, thus Mdm2 inhibitors are currently being evaluated in clinical trials as new anticancer drugs (Vassilev et al., 2004; Zhao et al., 2015). Based on these findings and of interest for our study, in MCF7 cells, a breast cancer cell line, a potential link between mTOR, Mdm2 and GRKs was suggested by the demonstration that, in response to the IGF-1 growth factor, Mdm2 phosphorylation by Akt kinase (which is part of the mTOR

pathway) stimulated GRK2 translocation from cytoplasm to nucleus and impaired Mdm2-dependent GRK2 degradation (Feng et al., 2004; Mayo and Donner 2001; Salcedo et al., 2006). Prompted by these findings, to investigate the potential involvement of Mdm2 in oligodendrogenesis, we demonstrated that, in immature OLs, a pool of endogenous GRK2 and Mdm2 indeed co-immunoprecipitated in the same molecular complex. More relevant, inhibition of mTOR by RAPA markedly increased GRK2/Mdm2 association. Moreover, likely due to Mdm2 increased availability, disruption of the p53-Mdm2 complex by Nutlin-3 potentiated GRK2/Mdm2 association, sequentially leading to (i) decreased GRK2 levels, (ii) reduced GRK2-GPR17 interaction after LTD<sub>4</sub> stimulation, (iii) inhibition of LTD<sub>4</sub>-induced GPR17 desensitization and, (iv) impaired OPC maturation. These effects were specific for LTD<sub>4</sub>, since Nutlin-3 did not affect UDP-glucose-induced GPR17 desensitization. Based on these data, we speculate that, similarly to other disorders (i.e., rheumatoid arthritis (Lombardi et al., 1999; Taranto et al., 2005), low levels of GRK2 under demyelinating conditions may be due to a primary functional change of Mdm2, thus unveiling this ligase as a new player in OPCs terminal differentiation.

### **Acknowledgements**

This research was supported by Fondazione Italiana Sclerosi Multipla grant 2013/R/1 to MPA. DL was supported by the Umberto Veronesi Foundation (2014). Authors thank Patrizia Rosa for kindly providing the home-made anti-GPR17 antibody, Carla Taveggia for help in the set up of OPC-DRG co-culture model, and Paolo Gelosa for technical assistance with the *in vivo* treatment. The authors declare no conflicts of interest.

## References

- Arva NC, Talbott KE, Okoro DR, Brekman A, Qiu WG, Bargonetti J. 2008. Disruption of the p53-Mdm2 complex by Nutlin-3 reveals different cancer cell phenotypes. *Ethn Dis* 18:S2-1-8.
- Ashcroft M, Vousden KH. 1999. Regulation of p53 stability. *Oncogene* 18:7637-43.
- Boda E, Vigano F, Rosa P, Fumagalli M, Labat-Gest V, Tempia F, Abbracchio MP, Dimou L, Buffo A. 2011. The GPR17 receptor in NG2 expressing cells: focus on in vivo cell maturation and participation in acute trauma and chronic damage. *Glia* 59:1958-73.
- Caccamo A, Majumder S, Richardson A, Strong R, Oddo S. 2010. Molecular interplay between mammalian target of rapamycin (mTOR), amyloid-beta, and Tau: effects on cognitive impairments. *J Biol Chem* 285:13107-20.
- Ceruti S, Vigano F, Boda E, Ferrario S, Magni G, Boccazzi M, Rosa P, Buffo A, Abbracchio MP. 2011. Expression of the new P2Y-like receptor GPR17 during oligodendrocyte precursor cell maturation regulates sensitivity to ATP-induced death. *Glia* 59:363-78.
- Chen Y, Wu H, Wang S, Koito H, Li J, Ye F, Hoang J, Escobar SS, Gow A, Arnett HA and others. 2009. The oligodendrocyte-specific G protein-coupled receptor GPR17 is a cell-intrinsic timer of myelination. *Nat Neurosci* 12:1398-406.
- Ciana P, Fumagalli M, Trincavelli ML, Verderio C, Rosa P, Lecca D, Ferrario S, Parravicini C, Capra V, Gelosa P and others. 2006. The orphan receptor GPR17 identified as a new dual uracil nucleotides/cysteinyl-leukotrienes receptor. *EMBO J* 25:4615-27.
- Cobelens PM, Kavelaars A, Heijnen CJ, Ribas C, Mayor F, Jr., Penela P. 2007. Hydrogen peroxide impairs GRK2 translation via a calpain-dependent and cdk1-mediated pathway. *Cell Signal* 19:269-77.
- Coppi E, Maraula G, Fumagalli M, Failli P, Cellai L, Bonfanti E, Mazzoni L, Coppini R, Abbracchio MP, Pedata F and others. 2013. UDP-glucose enhances outward K(+) currents necessary for cell differentiation and stimulates cell migration by activating the GPR17 receptor in oligodendrocyte precursors. *Glia* 61:1155-71.
- Daniele S, Trincavelli ML, Fumagalli M, Zappelli E, Lecca D, Bonfanti E, Campiglia P, Abbracchio MP, Martini C. 2014. Does GRK-beta arrestin machinery work as a "switch on" for GPR17-mediated activation of intracellular signaling pathways? *Cell Signal* 26:1310-25.
- Feng J, Tamaskovic R, Yang Z, Brazil DP, Merlo A, Hess D, Hemmings BA. 2004. Stabilization of Mdm2 via decreased ubiquitination is mediated by protein kinase B/Akt-dependent phosphorylation. *J Biol Chem* 279:35510-7.
- Franklin RJ, Ffrench-Constant C. 2008. Remyelination in the CNS: from biology to therapy. *Nat Rev Neurosci* 9:839-55.
- Fratangeli A, Parmigiani E, Fumagalli M, Lecca D, Benfante R, Passafaro M, Buffo A, Abbracchio MP, Rosa P. 2013. The regulated expression, intracellular trafficking and

membrane recycling of the P2Y-like receptor GPR17 in Oli-neu oligodendroglial cells. *J Biol Chem*.

Freedman DA, Wu L, Levine AJ. 1999. Functions of the MDM2 oncoprotein. *Cell Mol Life Sci* 55:96-107.

Fumagalli M, Daniele S, Lecca D, Lee PR, Parravicini C, Fields RD, Rosa P, Antonucci F, Verderio C, Trincavelli ML and others. 2011. Phenotypic changes, signaling pathway, and functional correlates of GPR17-expressing neural precursor cells during oligodendrocyte differentiation. *J Biol Chem* 286:10593-604.

Guardiola-Diaz HM, Ishii A, Bansal R. 2012. Erk1/2 MAPK and mTOR signaling sequentially regulates progression through distinct stages of oligodendrocyte differentiation. *Glia* 60:476-86.

Gurevich EV, Tesmer JJ, Mushegian A, Gurevich VV. 2012. G protein-coupled receptor kinases: more than just kinases and not only for GPCRs. *Pharmacol Ther* 133:40-69.

Hamano K, Iwasaki N, Takeya T, Takita H. 1996. A quantitative analysis of rat central nervous system myelination using the immunohistochemical method for MBP. *Brain Res Dev Brain Res* 93:18-22.

Kuhlmann T, Miron V, Cui Q, Wegner C, Antel J, Bruck W. 2008. Differentiation block of oligodendroglial progenitor cells as a cause for remyelination failure in chronic multiple sclerosis. *Brain* 131:1749-58.

Lecca D, Trincavelli ML, Gelosa P, Sironi L, Ciana P, Fumagalli M, Villa G, Verderio C, Grumelli C, Guerrini U and others. 2008. The recently identified P2Y-like receptor GPR17 is a sensor of brain damage and a new target for brain repair. *PLoS One* 3:e3579.

Lombardi MS, Kavelaars A, Schedlowski M, Bijlsma JW, Okihara KL, Van de Pol M, Ochsmann S, Pawlak C, Schmidt RE, Heijnen CJ. 1999. Decreased expression and activity of G-protein-coupled receptor kinases in peripheral blood mononuclear cells of patients with rheumatoid arthritis. *FASEB J* 13:715-25.

Mayo LD, Donner DB. 2001. A phosphatidylinositol 3-kinase/Akt pathway promotes translocation of Mdm2 from the cytoplasm to the nucleus. *Proc Natl Acad Sci U S A* 98:11598-603.

Narayanan SP, Flores AI, Wang F, Macklin WB. 2009. Akt signals through the mammalian target of rapamycin pathway to regulate CNS myelination. *J Neurosci* 29:6860-70.

Salcedo A, Mayor F, Jr., Penela P. 2006. Mdm2 is involved in the ubiquitination and degradation of G-protein-coupled receptor kinase 2. *EMBO J* 25:4752-62.

Taranto E, Xue JR, Lacey D, Hutchinson P, Smith M, Morand EF, Leech M. 2005. Detection of the p53 regulator murine double-minute protein 2 in rheumatoid arthritis. *J Rheumatol* 32:424-9.

Thut CJ, Goodrich JA, Tjian R. 1997. Repression of p53-mediated transcription by MDM2: a dual mechanism. *Genes Dev* 11:1974-86.

Tyler WA, Gangoli N, Gokina P, Kim HA, Covey M, Levison SW, Wood TL. 2009. Activation of the mammalian target of rapamycin (mTOR) is essential for oligodendrocyte differentiation. *J Neurosci* 29:6367-78.

Tyler WA, Jain MR, Cifelli SE, Li Q, Ku L, Feng Y, Li H, Wood TL. 2011. Proteomic identification of novel targets regulated by the mammalian target of rapamycin pathway during oligodendrocyte differentiation. *Glia* 59:1754-69.

Vassilev LT, Vu BT, Graves B, Carvajal D, Podlaski F, Filipovic Z, Kong N, Kammlott U, Lukacs C, Klein C and others. 2004. In vivo activation of the p53 pathway by small-molecule antagonists of MDM2. *Science* 303:844-8.

Vroon A, Kavelaars A, Limmroth V, Lombardi MS, Goebel MU, Van Dam AM, Caron MG, Schedlowski M, Heijnen CJ. 2005. G protein-coupled receptor kinase 2 in multiple sclerosis and experimental autoimmune encephalomyelitis. *J Immunol* 174:4400-6.

Zappelli E, Daniele S, Abbracchio MP, Martini C, Trincavelli ML. 2014. A rapid and efficient immunoenzymatic assay to detect receptor protein interactions: G protein-coupled receptors. *Int J Mol Sci* 15:6252-64.

Zhao Y, Aguilar A, Bernard D, Wang S. 2015. Small-Molecule Inhibitors of the MDM2-p53 Protein-Protein Interaction (MDM2 Inhibitors) in Clinical Trials for Cancer Treatment. *J Med Chem* 58:1038-52.

## Figure legends

### **Figure 1. mTOR inhibition by rapamycin impairs OPC maturation and increases GPR17 protein levels.**

(A) The scheme shows the experimental protocol of RAPA treatment and the different stages of OPC differentiation, starting from early oligodendrocyte precursors (stage 1) to mature OLs (stage 5). RAPA treatment was started at day 1 and differentiation media with or without RAPA was replenished every 72h. In most cases, analysis was performed at stage 4 and 5 (red circles); the outcome of these experiments is shown in the text. (B) Primary purified OPCs were cultured in the presence of PDGF and of bFGF for two days. Cell differentiation was induced by adding T3 to the medium. RAPA (15 nM) was added at day 1 and day 4. At day 6 (mature OLs, stage 5), cells were fixed for ICC analysis or lysed for WB analysis. Representative images of CTRL and RAPA treated-cells, showing double immunostaining with anti-GPR17 (green) and anti-MBP (red) antibodies. Histograms show the quantification of the percentage of GPR17 and MBP positive cells in control and treated cells (with vehicle-treated control cells set to 100%). Hoechst 33258 was used to label cell nuclei. The number of positive cells was counted in 10 optical fields under a 20X magnification. Data are the mean  $\pm$  S.E. of cell counts from a total of 3 coverslips/condition from three independent experiments,  $**p < 0.01$ ;  $***p < 0.001$  compared to CTRL, Student t-test. (C) Representative immunoblots of GPR17, CNPase and MBP protein levels in CTRL and RAPA treated-cells. Histograms show the results of densitometric analysis. Scanning densitometry was quantified and normalized to control (set to 100%) on the same WB.  $\alpha$ -tubulin expression was analysed from the same samples as an internal control. Data are expressed as mean  $\pm$  S.E. of three independent experiments.  $*p < 0.05$ ;  $**p < 0.01$ ; compared to CTRL, non parametric Mann-Whitney test. (D) Primary OPCs were transfected with a GPR17-EGFP fusion vector for GPR17 over-expression or with the control plasmid (containing EGFP only). After 48/72h, cells were fixed and stained for CNPase

(red). Scale bar 20 $\mu$ m. The percentage of transfected cells expressing CNPase over the total transfected cell population in the two conditions analysed was shown in the histogram. Forced GPR17 over-expression throughout differentiation stages significantly impairs spontaneous cell maturation  $***p < 0.001$  compared to control, Student's t-test, from 4 independent experiments.

**Figure 2. GRK2 plays a key role in mTOR regulation of GPR17 function and OL maturation.** (A) Representative immunoblots of GRK2 protein levels in CTRL and in RAPA treated cells. Histograms show the result of densitometric analysis. Scanning densitometry was quantified and normalized to control (set to 100%) on the same WB.  $\alpha$ -tubulin expression was analysed from the same samples as an internal control. Data from two independent experiments were shown (mean  $\pm$  S.E.,  $*p < 0.05$  compared to CTRL, non parametric Mann-Whitney test). (B) Primary OPCs were treated with medium alone (basal), 5  $\mu$ M UDP-glucose, or 50 nM LTD<sub>4</sub>, in the absence (CTRL) or in the presence of 15 nM RAPA. Cell lysates (30  $\mu$ g) were captured on wells pre-coated with anti-GPR17 antibody. After extensive washes, levels of GPR17/GRK2 complexes were quantified using a specific anti-GRK2 antibody. Data are the mean  $\pm$  S.E. of two independent experiments. One-way ANOVA followed by Bonferroni post-test:  $*p < 0.05$ ,  $***p < 0.001$  vs. basal value. (C) OPCs, isolated and differentiated at pre-oligodendrocytes (stage 3), were treated with 50 nM LTD<sub>4</sub> for different times (5-120 min), in the absence (white bars, CTRL) or in the presence (black bars) of 15 nM RAPA. After extensive washing, cells were treated for 15 min with 10  $\mu$ M FK, in the absence or in the presence of 5 nM LTD<sub>4</sub>. Intracellular cAMP levels were evaluated as reported in Materials and Methods. Data are expressed as the percentage of FK-stimulated cAMP levels, set to 100%, and represent the mean  $\pm$  S.E. of three independent experiments:  $*p < 0.05$ ,  $***p < 0.001$  vs LTD<sub>4</sub> stimuli,  $\#p < 0.05$ ,  $###p < 0.001$  vs relative

control cells, one-way ANOVA followed by Bonferroni post-test. (D) OPCs were electroporated with a GRK2 encoding plasmid. GRK2 over-expression was verified by WB (see the representative immunoblots). 30 h after transfection, cells were treated with 50 nM LTD<sub>4</sub> for different times (30-120 min), in the absence (white bars, CTRL) or presence of 15 nM RAPA (black bars). After extensive washing, cells were treated for 15 min with 10 μM FK, in the absence or in the presence of 5 nM LTD<sub>4</sub> and intracellular cAMP levels were evaluated. Data are expressed as the percentage of FK-stimulated cAMP levels, set to 100%, and represent the mean ± S.E. of two independent experiments. \**p* < 0.05, \*\**p* < 0.01, \*\*\**p* < 0.001 vs LTD<sub>4</sub> stimuli, one-way ANOVA followed by Bonferroni post-test.

**Figure 3. The ubiquitin ligase Mdm2 mediates the interaction between GRK2 and mTOR.** Primary OPCs were pre-incubated for 15 min with 15 nM RAPA (A) or 10 μM NUT (B) and treated with medium alone (basal), or UDP-glucose (5 μM) or with LTD<sub>4</sub> (50 nM), respectively for 30 min. Cell lysates (30 μg) were captured on wells pre-coated with anti-Mdm2 antibody. After extensive washes, levels of Mdm2/GRK complexes were quantified using specific anti-GRK2 or anti-GRK5 antibodies, and subsequently an HRP-conjugated antibody/TMB substrate kit. Blank wells were obtained in the absence of the primary anti-GRK antibodies. Data are expressed as fold vs. basal, and represent the mean ± S.E. of at least three independent experiments. \*\**p* < 0.01; \*\*\**p* < 0.001 vs. basal value, one-way ANOVA with Bonferroni post-test. (C) Primary OPCs (stage 3) were treated with medium alone (CTRL) or 15 nM RAPA for 30 min. At the end of the treatment period, cytosolic and nuclear fractions were collected. Representative immunoblots of Mdm2 levels in CTRL and in RAPA-treated cells. Histograms show the result of densitometric analysis. Scanning densitometry was quantified and normalized to control (set to 100%) on the same WB. α-actin and histone H3 expression were analysed from the same samples as loading controls

for the cytosolic and nuclear fraction, respectively. Data are expressed as mean  $\pm$  S.E. of two independent experiments. One-way ANOVA followed by Bonferroni post-test: \*\*\* $p$  < 0.001 compared to CTRL. (D) Representative immunoblots of GRK2 and GPR17 and CNPase protein levels in CTRL and in Nutlin-3 (NUT) treated cells. Histograms show the result of densitometric analysis. Scanning densitometry was quantified and normalized to control (set to 100%) on the same WB.  $\alpha$ -tubulin expression was analysed from the same samples as an internal control. Data are expressed as mean  $\pm$  S.E. of two independent experiments, \* $p$  < 0.05 compared to CTRL, non parametric Mann-Whitney test. (E) Primary OPCs were treated with medium alone (basal), 5  $\mu$ M UDP-glucose, or 50 nM LTD<sub>4</sub>, in the absence (control) or in the presence of 10  $\mu$ M NUT. Cell lysates (30  $\mu$ g) were captured on wells pre-coated with anti-GPR17 antibody. After extensive washes, levels of GPR17/GRK complexes were quantified using a specific anti-GRK2 antibody. Data are the mean  $\pm$  S.E. of two independent experiments. Statistical significance was determined with a one-way ANOVA with Bonferroni post-test: \* $p$  < 0.05, \*\*\* $p$  < 0.001 vs. basal value; # $p$  < 0.05, ## $p$  < 0.01, ### $p$  < 0.001 vs. respective CTRL.

**Figure 4. Sequestration of GRK2 by Mdm2 prevents GPR17 desensitization and OL maturation.** (A) OPCs, isolated and differentiated at pre-oligodendrocytes (stage 3), were treated with 50 nM LTD<sub>4</sub> or 5  $\mu$ M UDP-glucose (B) for different times (5-120 min), in the absence (white bars, CTRL) or presence of 10  $\mu$ M NUT (black bars). After extensive washing, cells were treated for 15 min with 10  $\mu$ M FK, in the absence or in the presence of 500 nM UDP-glucose or 5 nM LTD<sub>4</sub> and intracellular cAMP levels were evaluated. Data are expressed as the percentage of FK-stimulated cAMP levels, set to 100%, and represent the mean  $\pm$  S.E. of three independent experiments. \* $p$  < 0.05, \*\* $p$  < 0.01, \*\*\* $p$  < 0.001 vs UDP-glucose or LTD<sub>4</sub> stimuli, one-way ANOVA followed by Bonferroni post-test. (C) Primary

purified OPCs were cultured in the presence of PDGF and of bFGF for two days. Cell differentiation was induced by adding T3 to the medium. NUT (1  $\mu$ M) was added at day 1, 30 minutes before treating cells with LTD<sub>4</sub> (100 nM) or with vehicle. The differentiation degree of cells was monitored by analysing the number of cells expressing MBP at stage 4. Representative images of control (CTRL), NUT, LTD<sub>4</sub> and NUT+LTD<sub>4</sub> showing immunostaining with anti-MBP antibody (red). Histograms show the quantification of the percentage of MBP<sup>+</sup> cells in control and treated cells (with vehicle-treated control cells set to 100%). Hoechst 33258 was used to label cell nuclei. The number of MBP<sup>+</sup>-cells was counted in the entire coverslip under a 40X magnification. Data are the mean  $\pm$  S.E. of cell counts from a total of 3 coverslips/condition from three independent experiments \**p* <0.05; \*\**p* <0.01 compared to CTRL, ###*p* <0.01 compared to LTD<sub>4</sub>, non parametric Mann-Whitney test.

**Figure 5. Postnatal in vivo mTOR inhibition with rapamycin alters the normal development of GPR17, GRK2 and myelin associated proteins.** (A) The drawing shows the experimental plan for the in vivo treatment. C57BL6/J mice were injected daily with either vehicle (3 animals) or rapamycin (3 animals) intraperitoneally at a dose of 10 mg/kg body weight, starting from postnatal day (P) 16 to P20. On P21, mice were sacrificed, brains extracted, rapidly frozen at -80°C and processed for western-blot analysis. (B) Representative immunoblots of phospho-mTOR, mTOR, GPR17, GRK2, CNPase and MBP protein levels in control (CTRL) and rapamycin (RAPA) treated mice. Histograms show the result of densitometric analysis. Scanning densitometry was quantified and normalized to control condition (set to 100%) on the same western blot membrane.  $\alpha$ -tubulin expression was analysed from the same samples as an internal control. Data are expressed as mean  $\pm$  S.E. \**p* <0.05; compared to CTRL, non parametric Mann-Whitney test.

**Figure 6.** A cartoon illustrating the signalling pathways involved in GPR17 desensitization/down-regulation and OPC maturation. (A) Under conditions leading to physiological activation of the mTOR pathway, Mdm2 is mainly associated to the nucleus and bound to p53 and does not interfere with GRK2-mediated GPR17 desensitization in response to LTD<sub>4</sub>. (B) Inhibition of mTOR by rapamycin induced a redistribution of the intracellular concentrations of Mdm2, reducing its nuclear interaction with p53 and increasing the Mdm2/GRK2 association, causing a reduction of the expression levels of GRK2 and a subsequent loss in GPR17 desensitization in response to LTD<sub>4</sub>. The latter event impairs OPC maturation. To confirm the role of Mdm2 in GPR17 desensitization, Nutlin-3, releasing Mdm2 from its complex with p53, favoured the degradation of GRK2 mediated by Mdm2 and contributed to the impairment in thus impairing GPR17 desensitization and OPC maturation.

**The ubiquitin ligase Mdm2 controls oligodendrocyte maturation by intertwining mTOR  
with G protein-coupled receptor kinase 2 in the regulation of GPR17 receptor  
desensitization**

Marta Fumagalli<sup>a,\*</sup>, Elisabetta Bonfanti<sup>a,\*</sup>, Simona Daniele<sup>b</sup>, Elisa Zappelli<sup>b</sup>, Davide Lecca<sup>a</sup>,  
Claudia Martini<sup>b</sup>, Maria L. Trincavelli<sup>b</sup>, Maria P. Abbracchio<sup>a</sup>

\*These authors equally contributed to the present study

<sup>a</sup>Department of Pharmacological and Biomolecular Sciences, Università degli Studi di  
Milano, 20133 Milan, Italy.

<sup>b</sup>Department of Pharmacy, University of Pisa, 56126 Pisa, Italy.

**Running title:** Mdm2 controls myelination regulating GPR17

**Number of words:**

Abstract:	151
Introduction:	461
Materials and Methods:	1,893
Results:	2,016
Discussion:	711
Acknowledgements:	63
References:	1003
Figure Legends:	1,747
Number of Figures	6 (+ 5 Supplementary Figures)

TOTAL WORD COUNT (including title page) : 8055

**Corresponding Author**

Prof. Maria P. Abbracchio

Department of Pharmacological and Biomolecular Sciences, University of Milan, via Balzaretti 9, 20133 Milan, Italy. Tel: +390250318304; Fax: +390250318284;

E-mail: mariapia.abbracchio@unimi.it

**Main points**

- Untimely upregulation of GPR17 impairs oligodendrocyte maturation and myelination
- Mdm2 regulates GPR17 responses at the cell membrane by intertwining mTOR with GRK2
- Unprecedented role for Mdm2 ubiquitin ligase in oligodendrogenesis and myelination

**Keywords:** GPR17 receptor; oligodendrocyte precursor cells; myelination; rapamycin; Nutlin-3

**Abstract**

During oligodendrocyte precursor cell (OPC) differentiation, defective control of the membrane receptor GPR17 has been suggested to block cell maturation and impair remyelination under de-myelinating conditions.

After the immature oligodendrocyte stage, to enable cells to complete maturation, GPR17 is physiologically down-regulated via phosphorylation/desensitization by G protein-coupled Receptor Kinases (GRKs); conversely, GRKs are regulated by the “mammalian target of rapamycin” mTOR. However, how GRKs and mTOR are connected to each other in modulating GPR17 function and oligodendrogenesis has remained elusive.

Here we show, for the first time, a role for Murine double minute 2 (Mdm2), a ligase previously involved in ubiquitination/degradation of the onco-suppressor p53 protein. In maturing OPCs, both rapamycin and Nutlin-3, a small molecule inhibitor of Mdm2-p53 interactions, increased GRK2 sequestration by Mdm2, leading to impaired GPR17 down-regulation and OPC maturation block. Thus, Mdm2 intertwines mTOR with GRK2 in regulating GPR17 and oligodendrogenesis and represents a novel actor in myelination.

## Introduction

Remyelination after central nervous system (CNS) insults is needed to re-establish nerve conduction and prevent axonal loss. Spontaneous remyelination based on recruitment and proliferation of oligodendrocyte precursor cells (OPCs) is defective in diseases such as multiple sclerosis, mainly due to an OPC differentiation block (Franklin and Ffrench-Constant 2008; Kuhlmann et al., 2008). Identifying the mechanisms involved in defective OPC differentiation is important for developing new remyelinating strategies.

The P2Y-like GPR17 receptor responding to uracil-nucleotides and cysteinyl-leukotrienes (cysLTs), two families of mediators involved in CNS repair (Ciana et al., 2006), is a key regulator of OPC maturation (Chen et al., 2009; Coppi et al., 2013; Lecca et al., 2008). GPR17 is expressed by a subpopulation of early OPCs and it is needed to start differentiation; however, GPR17 is turned down before cells reach maturation (Fumagalli et al., 2011). GPR17 responses are regulated by its endogenous ligands; by binding to the receptor, ligands first induce OPCs to undergo differentiation and then switch GPR17 off, inducing its desensitization/down-regulation and cytoplasmic internalization. These latter events involve specific isoforms of G-protein-coupled receptor kinases (GRKs), either GRK2 or GRK5, depending on the class of ligand bound to the receptor (Daniele et al., 2014). Alterations of GPR17 activation and physiological silencing at specific OPC differentiation phases may lead to myelination defects and be even at the basis of demyelinating diseases.

In various *in vivo* neurodegenerative models characterized by myelin loss (stroke, trauma, demyelination and experimental autoimmune encephalomyelitis), GPR17 was abnormally up-regulated in OPCs around lesion sites (Boda et al., 2011; Chen et al., 2009; Lecca et al., 2008). Accordingly, we recently reported that decreased GRKs levels resulting in defective GPR17 desensitization markedly reduce OPC maturation (Daniele et al., 2014). Of interest, altered GRKs expression/activity has been implicated in human inflammatory and demyelinating diseases (Gurevich et al., 2012; Vroon et al., 2005).

GRKs alterations may, in turn, depend on mTOR (the “mammalian target of rapamycin”), a serine/threonine protein-kinase inhibited by the immunosuppressive agent rapamycin (RAPA). mTOR is central to cell growth, differentiation and survival and has been implicated in oligodendrocyte (OL) development and myelination (Tyler et al., 2009). Interestingly, a recent proteomic analysis highlighted increased levels of GPR17 in RAPA-treated OPCs, suggesting this receptor as a putative target for mTOR (Tyler et al., 2011). Despite this initial evidence, the relationships between mTOR, GRKs, GPR17, its interacting proteins and OL maturation have remained elusive.

Here, we demonstrate that, in rat primary OPCs, inhibition of mTOR by RAPA reduces GRK2 levels and prevents GPR17 down-regulation/desensitization, strongly inhibiting OPC maturation. We also prove, for the first time, that Mdm2 (Murine double minute-2), a ligase previously involved in the ubiquitination/degradation of the onco-suppressive p53 protein and in tumor progression (Ashcroft and Vousden 1999) specifically controls OPC maturation by intertwining mTOR with GRK2.

## **Materials and Methods**

### **Oligodendrocyte precursor cell cultures**

Primary OPCs were isolated from mixed glial cultures prepared from postnatal day 2 Sprague–Dawley rat cortex by shaking cells on an orbital shaker at 200 rpm, as previously described (Fumagalli et al., 2011). OPCs were then collected and separated from microglia by incubation for 1h on an uncoated Petri dish. Purified OPCs were seeded onto poly-D,L-ornithine-coated glass coverlips or plates (50 µg/ml, Sigma-Aldrich, Milan, Italy) to a specific density according to the planned experiments (see below), in Neurobasal (Life Technologies, Monza, Italy) with 2% B27 (Life Technologies), 2 mM L-glutamine (EuroClone), 10 ng/ml human platelet-derived growth factor BB (Sigma-Aldrich), and 10

ng/ml human basic fibroblast growth factor (Space Import Export, Milan, Italy), to promote proliferation. After 2 day, cells were switched to a Neurobasal medium lacking growth factors to allow differentiation. In some experiments triiodothyronine T3 (Sigma Aldrich) was also added to a final concentration of 10 ng/ml.

### ***In vitro* pharmacological treatments**

According to the planned experiments, cells were plated in 13 mm glass coverslip or in 60 mm diameter petri dish (20,000 cells/coverslip or 100,000 cells/dish) maintained for 2 days in Neurobasal supplemented with B27 and proliferative factors (PDGF-BB and bFGF) and then, after one day in differentiating medium, cells were treated with either rapamycin (15 nM) (Sigma-Aldrich) or with Nutlin-3 (NUT, 1  $\mu$ M) (Sigma Aldrich). Cells were fixed for immunocytochemistry (ICC) or lysed for WB analysis at day 4 or 6 (see also figure legends for details).

### **Generation of pGPR17-EGFP-N1 plasmid and OPC transfection**

The coding sequence of the human GPR17 receptor was subcloned from a previously generated pcDNA3.1 vector (Life Technologies), using specific primers containing the restriction cassette for XhoI and BamHI (fw: 5'-gtttttctcgagatgaatggcctgaagtggc; rv: 5'-ggtggatccgacagctctgacttggcactca). The product was then inserted upstream to the EGFP sequence in a pEGFP-N1 expression vector (Clontech). For GPR17 over-expression in OPCs, cells were seeded on 13 mm poly-D,L-ornithine-coated coverslips ( $2 \times 10^4$  cells/well) in Neurobasal supplemented with B27 and proliferative factors (PDGF-BB and bFGF). Differentiation was then, induced by removing proliferative factors and at day 4, cells were transfected with the fluorescent plasmid pGPR17-EGFP, in parallel to the corresponding fluorescent empty vector, using the transfection reagent NeuroFECT<sup>TM</sup> (Genlantis, San

Diego, CA, USA) according to manufacturer's protocol. After transfection, cells were maintained in differentiating medium supplemented with T3 for additional 48-72 hours and fixed for ICC.

### **OPCs electroporation with a GRK2 plasmid**

GRK2 overexpression was obtained by electroporating OPCs with the Amaxa Rat Oligodendrocyte Nucleofection Kit (Lonza, Milan, Italy) according to the manufacture' instructions. In detail, OPCs were electroporated with 1 µg either of GRK2 plasmid (Origene) or the corresponding empty vector (OriGene, Maryland, USA) with the O-017 program. After electroporation, cells were rapidly seeded on 13 mm poly-D,L-ornithine-coated coverslips ( $5 \times 10^4$  cells/well) in Neurobasal supplemented with B27 and proliferative factors (PDGF-BB and bFGF) and maintained in this medium. In parallel, electroporated OPCs were also seeded on 60 mm poly-D,L-ornithine-coated dish in order to check transfection efficiency by western-blot analysis. After 30 hours, electroporated OPCs were subjected to the cAMP assay (see below)

### **Immunocytochemistry**

Both primary OPCs and OPC-DRG co-cultures were fixed at room temperature with 4% paraformaldehyde (Sigma-Aldrich) in 0.1 M PBS (Euroclone) containing 0.12 M sucrose (Sigma-Aldrich). Labelling was performed incubating cells overnight at 4°C with the following primary antibodies in Goat Serum Dilution Buffer (GSDB; 450 mM NaCl, 20 mM sodium phosphate buffer, pH 7.4, 15% goat serum, 0.3% Triton X-100): rat anti-MBP (1:200; Millipore, Milan, Italy), rabbit anti-GPR17 (1:100; Cayman, Michigan, USA), mouse anti-SMI 31 and mouse anti SMI 32 (1:500; Cell Signaling, Beverly, MA, USA). Cells were then incubated for 1h at RT with the secondary goat anti-rat, goat anti-rabbit or goat anti-mouse

antibody conjugated to Alexa Fluor 555 or Alexa Fluor 488 (1:600 in GSDB; Molecular Probes, Life Technologies). Nuclei were labelled Hoechst-33258 (1:10,000, Molecular Probes, Life Technologies). Coverslips were finally mounted with a fluorescent mounting medium (Dako, Milan, Italy) and analysed under a fluorescence or confocal microscope (LSM510 META, Zeiss). For cell count, 10 or 20 fields were acquired at 20X magnification (at least 3 coverslips for each experimental condition) under an inverted fluorescence microscope (200M; Zeiss) connected to a PC computer equipped with the Axiovision software (Zeiss). Images were collected and cells scored and counted using the ImageJ software.

### **Subcellular localization of Mdm2**

Primary OPCs (stage 3) were treated with medium alone (CTRL) or 15 nM RAPA for 30 min. At the end of treatments, cells were collected and suspended in 5 mM Tris-EDTA (pH 7.4) and nuclear cell fractions were isolated by centrifugation at 1000 x g for 15 min at 4°C. Mdm2 levels were detected in both cytoplasmic and nuclear fractions by immunoblotting using an anti-Mdm2 antibody (Santa Cruz Biotechnology, sc-812; 1:100). GAPDH (Sigma Aldrich, G9545, 1:5000) and histone H3 (Santa Cruz Biotechnology, sc-8654; 1:100) were analysed from the same samples as loading controls for the cytosolic and nuclear fraction, respectively.

### **Western blot analysis**

Cell lysates were prepared and analysed by WB as previously described (Coppi et al., 2013). Briefly, cells were lysed in lysis buffer (20 mM Tris pH 7.2, 0.5% deoxycholate, 1% Triton, 0.1% SDS, 150 mM NaCl, 1 mM EDTA and 1% proteases inhibitors, Sigma-Aldrich) and, then, approximately 25-30 µg aliquots from each protein sample were loaded on 12%

sodium-dodecylsulphate polyacrylamide gels (for MBP and CNPase) or on 8.5% sodium-dodecylsulphate polyacrylamide gels (for GPR17, NG2, GRK2 and GRK5), and blotted onto nitrocellulose membranes (MBP and CNPase) or PVDF membranes (GPR17, GRK2, GRK5 and NG2) (Bio-Rad Laboratories, Segrate, Milan, Italy). Membranes were saturated with 10% non-fat dry milk in Tris-buffered saline (TBS; 1 mM Tris-HCl, 15 mM NaCl, pH 8) for 1 h at room temperature and incubated overnight at 4°C with the following primary antibodies diluted in 5% non-fat dry milk in TBS: rabbit anti-GPR17 (1:1000, home-made antibody), rat anti-MBP (1:500), rabbit anti-CNPase (1:250; Santa Cruz Biotechnology, Santa Cruz, CA, USA), rabbit anti-GRK2 (sc-562, 1:200; Santa Cruz Biotechnology) and rabbit anti-GRK5 (sc-565, 1:200; Santa Cruz Biotechnology), rabbit anti-phospho mTOR (Ser2448) (1:500; Cell Signaling, Danvers, MA, USA), mouse anti-mTOR (1:1000; Cell Signaling). The following day, membranes were washed in TBS-T (TBS plus 0.1% Tween20® Sigma Aldrich), incubated for 1 h with goat anti-rabbit or goat anti-mouse or goat anti-rat secondary antibodies conjugated to horseradish peroxidase (1:4000, 1:2000 and 1:2000 in 5% non-fat dry milk in TBS respectively; Sigma-Aldrich). Detection of proteins was performed by enhanced chemiluminescence (ECL, Thermo Scientific, Rodano, Milan, Italy) and autoradiography. Non-specific reactions were evaluated in the presence of the secondary antibodies alone. Densitometric analysis of the protein bands was performed with ImageJ software. Band intensities were measured as integrated density volumes (IDV) and expressed as % of control lane values for comparisons between treatment groups.  $\alpha$ -Tubulin (1:1500; Sigma Aldrich) or  $\alpha$ -actin (1:5000; Sigma Aldrich) expression was analysed from the same sample as an internal control and it was used for data normalization.

### **Measurement of cyclic AMP levels**

For OPCs, cells were plated in 24 well-plates and after 6 days in culture in differentiation medium without T3, functional responsiveness of GPR17 was assessed as described, (Daniele et al., 2014; Fumagalli et al., 2011) using 500 nM UDP-glucose or 5 nM LTD<sub>4</sub>, as stimuli. For desensitisation experiments, OPCs were pre-treated with UDP-glucose (5 µM) or LTD<sub>4</sub> (50 nM) for different times (5-120 min), in the absence (control cells) or in the presence of 15 nM rapamycin or 10 µM Nutlin-3. Then, cells were washed with 400 µl of saline and incubated at 37°C for 15 min with 0.4 ml of non-complete Neurobasal in the presence of the phosphodiesterase inhibitor, Ro20-1724 (20 µM) and stimulated with agonists (500 nM UDP-glucose or 5 nM LTD<sub>4</sub>), in the presence of 10 µM Forskolin (FK). Intracellular cAMP levels were measured using a competitive protein binding method, as previously reported (Daniele et al., 2014).

#### **ELISA assay for the detection of GPR17-GRK or Mdm2-GRK immunocomplexes**

OPCs were treated with medium alone (basal), or UDP-glucose (5µM) or with LTD<sub>4</sub> (50 nM), respectively for 30 min. In some experiments, cells were pre-incubated for 15 min with 15 nM rapamycin or 10 µM Nutlin-3. Then, cells were washed twice in ice-cold phosphate-buffered saline, collected by centrifugation, and resuspended in Lysis buffer (20 mM Tris HCl, 137 mM NaCl, 10% glycerol, 1% NONIDET40, 2 mM EDTA, pH 8), containing 1% of the Protease inhibitor Cocktail (Sigma Aldrich, Milan, Italy). Optimal composition of lysis buffer, as well as reaction conditions, were determined in preliminary experiments. Levels of GPR17-GRK or Mdm2-GRK immunocomplexes in OPC lysates, obtained as above described, were quantified using a validated ELISA method (Zappelli et al., 2014). 96-wells were pre-coated with a mouse full-length anti-Mdm2 antibody (sc-965, Santa Cruz Biotechnology, 1:50 in 0.05% Poly-L-Ornithine) or with an anti-N terminus GPR17 antibody (sc-74792, Santa Cruz Biotechnology, 1:50 in 0.05% Poly-L-Ornithine) overnight at room

temperature. After three washes of 5 minutes with 100  $\mu$ l of PBS/Tween 0.1%, cell lysates (50  $\mu$ g in a final volume of 100  $\mu$ l) were transferred to the pre-coated wells for 120 min with a plastic cover or film and kept under constant agitation. Three quick washes were performed with PBS/Tween 0.1% to remove unbound protein, and each well was incubated for 15 min with 1% bovine serum albumin (BSA, Sigma) to block non-specific sites. Then, wells were incubated for 120 min at room temperature with the specific primary antibodies: anti-GRK2 (Santa Cruz Biotechnology, sc-562; 1:400); anti-GRK5 (Santa Cruz Biotechnology, sc-565; 1:400). Wells were washed and incubated for 1 h with a secondary HRP-conjugate antibody (diluted in 5% milk), and washed again. The TMB substrate kit (Thermo Fisher Scientific) allowed a colorimetric quantification of the complex of GRKs with GPR17 or Mdm2. Blanks were obtained processing cell lysates in the absence of the primary antibodies. To avoid cross interactions between the different antibodies, the chosen primary antibody was always from a different species with respect to the antibody used for well pre-coating. Absorbance's values at 450 nm were measured, background subtracted and bar graphs were generated using Graph Pad Prism 4 software (GraphPad Software Inc., San Diego, CA), from which the percentage of association between the two analysed proteins, compared to basal value, were derived.

#### **In vivo rapamycin injections.**

C57BL6/J mice were injected daily with either vehicle or rapamycin intraperitoneally at 10 mg/kg body weight (rapamycin was diluted in the vehicle solution from a stock of 20 mg/mL in 100% ethanol immediately before the injection to a final concentration of 0.8 mg/mL PBS, 5% polyethylene glycol-1000, 5% Tween 80, and 4% ethanol) starting at postnatal day (P) 16. On P21, mice were sacrificed, brains were extracted and rapidly frozen at  $-80^{\circ}\text{C}$ . Membrane protein extracts were obtained by tissue homogenization in lysis buffer (20 mM Tris pH 7.2, 0.5% deoxycholate, 1% Triton, 0.1% SDS, 150 mM NaCl, 1 mM EDTA and 1%

proteases inhibitors, Sigma-Aldrich). The homogenate was centrifuged at 1000g for 10 min at 4°C in order to eliminate nuclei. The protein concentration was estimated using the Bio-Rad Protein Assay (Bio-Rad Laboratories s.r.l., Segrate, Italy). Western blot analysis was performed as described below.

### **Statistical analysis**

All results were expressed as mean  $\pm$  S.E. Statistical analysis was done with non-linear multipurpose curve-fitting Graph-Pad Prism program (Graph-Pad). The statistical test used was chosen according to the type of experiment performed and was indicated in the legend of the figure. Three degrees of significance were considered:  $P < 0.05$  (\*),  $P < 0.01$  (\*\*),  $P < 0.001$  (\*\*\*)).

### **Results**

#### **Involvement of mTOR in GPR17 regulation during OPC differentiation**

Cultured OPCs are known to undergo different subsequent stages of differentiation (stages 1-5) when maintained for up to 6 days in vitro (DIV6) when they reach terminal maturation (stage 5 in Figure 1A). Initial data from a proteomic analysis had shown that RAPA increases GPR17 levels in parallel to a reduction of OPC maturation, highlighting GPR17 as a potential target for mTOR and suggesting that receptor silencing is required for OPC terminal maturation (Ceruti et al., 2011; Fumagalli et al., 2011; Lecca et al., 2008). To get more insights in mTOR regulation of GPR17 and on its effects on OPC maturation, as a first step, we performed a detailed immunocytochemical and western blot (WB) analysis of GPR17 in OPCs treated with RAPA from DIV1 and analysed at either DIV4 (Supplementary Figure S1A) or DIV6 (Figure 1B). At DIV6 (stage 5), RAPA markedly reduced the number of terminal MBP<sup>+</sup> OLs and concomitantly increased the number of GPR17<sup>+</sup> cells (Figure 1B).

No changes in total cell number were detected (CTRL:  $527.4 \pm 73.64$ ; RAPA:  $412.6 \pm 55.59$ , Hoechst 33258 staining). WB analysis confirmed a significant GPR17 enhancement in parallel with reduced mature myelin proteins (CNPase and MBP) (Figure 1C). As shown in Supplementary Figure S1A, in RAPA-treated cells, an increase (+38.7%) of GPR17 compared to CTRL was already detected at DIV4 (stage 4), together with reductions of CNPase and MBP. Conversely, RAPA had no effect on GPR17 at DIV3 (data not shown). To confirm that the effects of RAPA on OPC maturation indeed result in impairments of myelination, RAPA-treated cultures also showed a reduction of MBP<sup>+</sup> segments extending along neurofilament (NF)-positive axons in neuronal/OPC co-cultures (Supplementary Figure S1B). To univocally endorse that GPR17 down-regulation is needed for OPC terminal maturation, we then transfected OPCs with a fluorescence reporter plasmid for GPR17 over-expression (GPR17-EGFP). After 3 days, the majority of control OPCs incorporating the empty plasmid underwent maturation, as demonstrated by CNPase expression and large cytoplasmic areas with many branched processes (Figure 1D). Conversely, most OPCs incorporating the vector for GPR17 over-expression kept an immature morphology and showed reduced expression of both CNPase (Figure 1D) and MBP (data not shown). Thus, interference with GPR17 down-regulation resulting in permanently elevated GPR17 levels markedly impairs OPC differentiation.

### **GRK2 plays a key role in mTOR regulation of GPR17 function and OL maturation**

In other cells, mTOR regulates the expression/function of membrane GPCRs by modulating GRKs (Cobelens et al., 2007). We previously showed that, in OPCs, GRKs are involved in GPR17 desensitization/internalization induced by prolonged exposure to its agonists, and that, depending on the type of ligand (either LTD<sub>4</sub> or UDP-glucose), different GRKs (namely, GRK2 or GRK5) are preferentially recruited to regulate GPR17 functional

response (Daniele et al., 2014).

To establish a functional relationship between mTOR and GRK in OPCs, we analysed the expression profile of these GRK isoforms at DIV4 and DIV6 in control and RAPA-treated cells. RAPA significantly decreased GRK2 levels (Figure 2A), whereas no changes in GRK5 were observed (Supplementary Figure S3A). Then, based on previous data showing that GPR17 associates to GRK2 to a higher extent after LTD<sub>4</sub> compared to UDP-glucose (Daniele et al., 2014) (see also Figure 2B), we measured GPR17-GRK2 association in OPCs in absence or presence of RAPA, and after either LTD<sub>4</sub> or UDP-glucose exposure. Consistent with data in Figure 2A, association of GPR17 to GRK2 was significantly decreased by RAPA, particularly when LTD<sub>4</sub> was used to activate GPR17 (Figure 2B). GPR17 is coupled to Gi and its activation by agonists consequently results in marked inhibition of intracellular levels of cAMP (Fumagalli et al., 2011). Accordingly, in OPCs, LTD<sub>4</sub> potently reduces the increases of cAMP levels induced by the cyclase activator FK (Figure 2C). This Gi mediated effect was progressively lost in cells exposed to the agonist for prolonged time periods, suggesting receptor desensitization (white columns in Figure 2C). RAPA markedly prevented LTD<sub>4</sub> induced receptor desensitization despite an initial challenge with this agonist (black columns in Figure 2C), likely due to a decrease in GRK2 levels. In contrast, UDP-glucose, which activates the GRK5-dependent pathway (Daniele et al., 2014) still induced GPR17 desensitization with kinetics similar to control OPCs (Supplementary Figure S3B). These results suggest that mTOR regulates GRK2 which, in turn, mediates LTD<sub>4</sub>-induced GPR17 desensitization. To further confirm this hypothesis and unequivocally relate RAPA-induced decrease in GRK2 levels with loss of GPR17 desensitization, we performed “rescue experiments” by over-expressing GRK2 in OPCs. Electroporation of cells with a GRK2 plasmid indeed resulted in a marked increase of GRK2 protein levels compared to the corresponding empty vector, as shown by western blot analysis (Fig. 2D). To make sure that

electroporation had no effects on GPR17 desensitization kinetics, we analyzed LTD<sub>4</sub>-mediated loss of GPR17 function in cells electroporated with the corresponding empty vector. In a similar way to standard controls (Fig. 2C), pre-exposure of electroporated OPCs to LTD<sub>4</sub> gradually desensitized GPR17, and, as expected, this effect was prevented by inhibiting mTOR with rapamycin (Supplementary Figure S2). On the contrary, in OPCs electroporated with the GRK2 plasmid, RAPA was no longer able to prevent LTD<sub>4</sub>-induced GPR17 desensitization (black columns compared to white columns in Fig. 2D). Globally, these results confirm that: (i) GRK2 is very important for LTD<sub>4</sub>-induced GPR17 desensitization; (ii) mTOR normally controls GRK2 activation and GPR17 desensitization; (iii) inhibition of mTOR by RAPA results in prevention of GPR17 desensitization, but this effect is surmounted by GRK2 overexpression; (iv) GRK2 is downstream of mTOR in the pathway of GPR17 desensitization.

### **The ubiquitin ligase Mdm2 mediates the interaction between GRK2 and mTOR**

To gain insights into mTOR-mediated mechanisms governing GRK2 levels/activity in OPCs, we analysed the involvement of the ubiquitin ligase Mdm2. This ligase normally acts as a negative regulator of the onco-suppressor p53 protein, but has also been reported to regulate membrane GPCRs by promoting the degradation of GRK2 in cells other than OPC (Freedman et al., 1999; Salcedo et al., 2006; Thut et al., 1997). On this basis, we quantified Mdm2-association to either GRK2 or GRK5 after mTOR inhibition. RAPA significantly enhanced Mdm2 association to GRK2 with no changes in Mdm2-GRK5 complexes, confirming that, in OPCs, Mdm2 is selective for GRK2 (Figure 3A and Supplementary Figure S5). These data are consistent with decreased GRK2 (Figure 2A) and unaltered GRK5 levels in RAPA-treated OPC lysates (Supplementary Figure S3A). To more directly establish a functional link between Mdm2 and GRK2, we took advantage of Nutlin-3, a small-

molecule inhibitor of Mdm2-p53 interactions (Arva et al., 2008), thus making Mdm2 more available for association to GRK2. Nutlin-3 (NUT) markedly enhanced Mdm2-GRK2 association, with negligible effects on the formation of Mdm2-GRK5 complexes (Figure 3B and Supplementary Figure S5). Sequestration of GRK2 by Mdm2 indeed resulted in a marked reduction of GRK2 levels (Figure 3C), suggesting that Mdm2 drives the ubiquitination/degradation of this kinase. A parallel increase of GPR17 together with decreased CNPase levels was also detected after Nutlin-3 (Figure 3D). In line with these data, Nutlin-3 markedly reduced the association of GRK2 to GPR17 after OPC exposure to GPR17 agonists, with a more marked effect after LTD<sub>4</sub> (Figure 3E). Globally, these data suggest that, in OPCs, disruption of Mdm2-p53 interaction favours the association of Mdm2 to GRK2 and its subsequent degradation, thus impairing GRK2 interaction with GPR17 (Figure 3E).

#### **mTOR regulates the equilibrium between Mdm2-p53 and Mdm2-GRK2 complexes**

The above data suggest that mTOR signaling would shift the equilibrium from Mdm2-p53 association to Mdm2-GRK2 association, thereby allowing GRK2 to mediate GPR17 desensitization and OPC maturation. To substantiate this hypothesis, we directly assessed the association of Mdm2 to p53 upon RAPA treatment. As shown in Fig. S4, pre-treatment of OPCs with either RAPA or Nutlin-3 for 30 min reduced the association between Mdm2 and p53. Since in other cells (e.g MCF-7 cells) mTOR dependent phosphorylation of Mdm2 stimulates its translocation from the cytoplasm to the nucleus (Mayo et al., 2001; Feng et al., 2004; Salcedo et al., 2006), where it then associates to p53, we reasoned that mTOR inhibition by RAPA could result in reduced levels of nuclear Mdm2 and in elevated expression of cytosolic Mdm2, which in turn can bind to and ubiquitinate GRK2, thus promoting its degradation. To test this hypothesis, Mdm2 protein levels were quantified in the cytosolic and nuclear compartments of OPCs upon treatment with RAPA. Western-blot

analysis (Fig. 3C) showed that RAPA enhanced Mdm2 cytosolic levels while reducing its nuclear concentrations, thus promoting its association to GRK2 with obvious consequences on GPR17 desensitization.

### **Sequestration of GRK2 by Mdm2 prevents GPR17 desensitization and OL maturation**

We then reasoned that Nutlin-3 might also profoundly influence agonist-induced GPR17 desensitization and OPC terminal maturation. Hence, we exposed OPCs to LTD<sub>4</sub> for 5-120 min, a condition normally resulting in a time-dependent loss of GPR17 activity (Figure 2C), in absence or presence of Nutlin-3. As expected, in control treated cells (CTRL), prolonged exposure to LTD<sub>4</sub> resulted in progressive GPR17 desensitization (white columns in Figure 4A). In Nutlin-3-treated cells, GPR17 response to LTD<sub>4</sub> was fully preserved, confirming that under these conditions GRK2 is no longer available for GPR17 desensitization (black columns in Figure 4A). Conversely, in line with the inability of Mdm2 to associate to GRK5 (Figure 3B), UDP-glucose induced a similar time-dependent loss of GPR17 response in both the absence (CTRL) and presence of Nutlin-3 (white and black columns in Figure 4B). We conclude that dissociation of Mdm2-p53 complexes by Nutlin-3 enhances Mdm2-mediated GRK2 degradation, with consequent decreases of GRK2 levels and block of LTD<sub>4</sub>-induced GPR17 desensitization.

To establish whether these effects also correlate with OPC differentiation, cells were first exposed to Nutlin-3 and then treated with LTD<sub>4</sub> to promote OPC maturation. As expected, LTD<sub>4</sub> increased the number of mature MBP-positive cells (Figure 4C). In the presence of Nutlin-3, LTD<sub>4</sub>-induced OPC maturation was reduced (Figure 4C) in line with the block of GPR17 desensitization under these settings (Figure 4A). We also observed a small, but statistically significant, decrease of OPC maturation when Nutlin-3 was applied to cells in the absence of LTD<sub>4</sub> (Figure 4C), to suggest a modulation of the effects induced by

endogenous GPR17 agonists. These data confirm that: (i) increased Mdm2 association to GRK2 reduces the ability of this kinase to desensitize GPR17, and that (ii) the GRK2-GPR17 interaction is required to complete OPC maturation.

Overall, results show that the Mdm2 ligase intertwines mTOR with GRK2 in regulating the GPR17 receptor and OPC maturation, thus unveiling a totally unexpected role for Mdm2 in oligodendrogenesis and myelination (Figure 6).

### **Postnatal *in vivo* treatment with RAPA increases GPR17 levels and reduces both GRK2 and myelin proteins**

In rodents, myelination occurs in early postnatal life (Hamano et al., 1996) and is completed by post-natal day (P) 21. After birth, GPR17 expression is progressively increased to reach maximal peaks at P14 (Boda et al., 2011), after which it is progressively decreased reaching lower stable levels typical of adult life. Consistent with GPR17 anticipating myelination (Chen et al., 2009), massive myelin production followed the peak of GPR17<sup>+</sup> cell density (P7–P14) and occurred concomitantly with the decrease in GPR17<sup>+</sup> cell number (Boda et al., 2011). If the relationships between mTOR, GRK2 and GPR17 detected in cultured OPCs are physiologically relevant, an early *in vivo* postnatal inhibition of mTOR should affect the normal maturation pattern of myelin proteins and also impact on cerebral GPR17 levels. We thus treated mice with either vehicle or RAPA (10 mg/Kg) (Guardiola-Diaz et al., 2012) daily from P16 to P20 (Supplementary Figure S3A), a time window during which GPR17 starts to be down-regulated (Boda et al., 2011). As expected from literature data (Caccamo et al., 2010), RAPA-injected mice displayed a marked reduction of mTOR phosphorylation on Ser2448, to confirm that *in vivo* RAPA-treatment successfully inhibited mTOR activity (Figure 5). Under these conditions, a statistically significant increase in GPR17 levels was found in parallel to a reduction of both GRK2 and mature myelin proteins

like CNPase and MBP (Figure 5B). These data fully confirm *in vivo* the relationships between mTOR, GRK2, GPR17 and myelination, suggesting that mTOR regulates postnatal myelination by fine-tuning GPR17 levels and that GPR17 phosphorylation/desensitization by GRK2 is crucially involved in physiological myelination.

## Discussion

Here we show, for the first time, a role of the ubiquitin ligase Mdm2 in oligodendrogenesis and myelination. Specifically, we demonstrate that Mdm2 intertwines the mammalian target of RAPA, mTOR, and the receptor kinase GRK2 in regulating the desensitization/inactivation of the GPR17 receptor, a key actor in OPC maturation to myelinating phenotypes.

Our previous studies highlighted GPR17 as an indispensable player in initiating OPC differentiation but also suggested down-regulation of the receptor is needed to complete cells' maturation. Our previous studies also demonstrated that GPR17 down-regulation occurs via agonist-induced receptor internalization, leading to a very marked degradation of the agonist-receptor complex in lysosomes and only partial re-recycling of GPR17 to the plasma membrane. The amount of internalized degraded receptor increased as a function of time of agonist exposure, suggesting that receptor re-routing to the membrane may be rather limited after long exposure times and/or at high agonist concentrations (Fratangeli et al., 2013).

Here, we first unequivocally confirmed that (Chen et al., 2009; Daniele et al., 2014) in cultured OPCs, forced GPR17 expression throughout their entire differentiation cycle impairs cells' maturation. Accordingly, mice aberrantly over-expressing GPR17 under the control of the promoter of CNPase, a relatively late stage marker, displayed myelin dysfunctions, tremors and precocious death (Chen et al., 2009). Moreover, in various neurodegeneration

animal models, OPCs over-expressing GPR17 accumulate at lesion sites (Boda et al., 2011; Chen et al., 2009; Lecca et al., 2008).

We then showed that RAPA-induced mTOR inhibition resulting in aberrant GPR17 up-regulation and reduced OPC differentiation is mediated by GRK2. Indeed, in late OPCs, a reduction of GRK2 expression/activity by RAPA impaired both GPR17 desensitization and OPC maturation (Daniele et al., 2014), suggesting that loss of this kinase (that normally phosphorylates and down-regulates membrane receptors) may be responsible for the persistent GPR17 up-regulation (Daniele et al., 2014). To support the relevance of these findings to an *in vivo* situation, postnatal treatment of mice with RAPA induced a cortical reduction of myelin-related proteins MBP and CNPase, confirming that mTOR signalling is required during myelination active phases (Narayanan et al., 2009). These effects were associated to an *in vivo* increase of GPR17 levels and a reduction of GRK2, suggesting a failure of GPR17 down-regulation, likely due to loss of mTOR control on GRK2. Of course, since mTOR is such a central signaling hub affecting simultaneously many different pathways, we cannot exclude that, especially *in vivo*, RAPA is also inducing other effects.

The crosstalk between mTOR and GRKs (Cobelens et al., 2007; Salcedo et al., 2006) in OPCs has never been investigated before. To address this issue, we focused on Mdm2, an ubiquitin ligase known for controlling p53 degradation and cancer malignancy (Ashcroft and Vousden 1999). In various types of human cancers, Mdm2 serves as an ubiquitin ligase that promotes p53 degradation, thus Mdm2 inhibitors are currently being evaluated in clinical trials as new anticancer drugs (Vassilev et al., 2004; Zhao et al., 2015). Based on these findings and of interest for our study, in MCF7 cells, a breast cancer cell line, a potential link between mTOR, Mdm2 and GRKs was suggested by the demonstration that, in response to the IGF-1 growth factor, Mdm2 phosphorylation by Akt kinase (which is part of the mTOR pathway) stimulated GRK2 translocation from cytoplasm to nucleus and impaired Mdm2-

dependent GRK2 degradation (Feng et al., 2004; Mayo and Donner 2001; Salcedo et al., 2006). Prompted by these findings, to investigate the potential involvement of Mdm2 in oligodendrogenesis, we demonstrated that, in immature OLS, a pool of endogenous GRK2 and Mdm2 indeed co-immunoprecipitated in the same molecular complex. More relevant, inhibition of mTOR by RAPA markedly increased GRK2/Mdm2 association. Moreover, likely due to Mdm2 increased availability, disruption of the p53-Mdm2 complex by Nutlin-3 potentiated GRK2/Mdm2 association, sequentially leading to (i) decreased GRK2 levels, (ii) reduced GRK2-GPR17 interaction after LTD<sub>4</sub> stimulation, (iii) inhibition of LTD<sub>4</sub>-induced GPR17 desensitization and, (iv) impaired OPC maturation. These effects were specific for LTD<sub>4</sub>, since Nutlin-3 did not affect UDP-glucose-induced GPR17 desensitization. Based on these data, we speculate that, similarly to other disorders (i.e., rheumatoid arthritis (Lombardi et al., 1999; Taranto et al., 2005), low levels of GRK2 under demyelinating conditions may be due to a primary functional change of Mdm2, thus unveiling this ligase as a new player in OPCs terminal differentiation.

### Acknowledgements

This research was supported by Fondazione Italiana Sclerosi Multipla grant 2013/R/1 to MPA. DL was supported by the Umberto Veronesi Foundation (2014). Authors thank Patrizia Rosa for kindly providing the home-made anti-GPR17 antibody, Carla Taveggia for help in the set up of OPC-DRG co-culture model, and Paolo Gelosa for technical assistance with the *in vivo* treatment. The authors declare no conflicts of interest.

## References

- Arva NC, Talbott KE, Okoro DR, Brekman A, Qiu WG, Bargonetti J. 2008. Disruption of the p53-Mdm2 complex by Nutlin-3 reveals different cancer cell phenotypes. *Ethn Dis* 18:S2-1-8.
- Ashcroft M, Vousden KH. 1999. Regulation of p53 stability. *Oncogene* 18:7637-43.
- Boda E, Vigano F, Rosa P, Fumagalli M, Labat-Gest V, Tempia F, Abbracchio MP, Dimou L, Buffo A. 2011. The GPR17 receptor in NG2 expressing cells: focus on in vivo cell maturation and participation in acute trauma and chronic damage. *Glia* 59:1958-73.
- Caccamo A, Majumder S, Richardson A, Strong R, Oddo S. 2010. Molecular interplay between mammalian target of rapamycin (mTOR), amyloid-beta, and Tau: effects on cognitive impairments. *J Biol Chem* 285:13107-20.
- Ceruti S, Vigano F, Boda E, Ferrario S, Magni G, Boccazzi M, Rosa P, Buffo A, Abbracchio MP. 2011. Expression of the new P2Y-like receptor GPR17 during oligodendrocyte precursor cell maturation regulates sensitivity to ATP-induced death. *Glia* 59:363-78.
- Chen Y, Wu H, Wang S, Koito H, Li J, Ye F, Hoang J, Escobar SS, Gow A, Arnett HA and others. 2009. The oligodendrocyte-specific G protein-coupled receptor GPR17 is a cell-intrinsic timer of myelination. *Nat Neurosci* 12:1398-406.
- Ciana P, Fumagalli M, Trincavelli ML, Verderio C, Rosa P, Lecca D, Ferrario S, Parravicini C, Capra V, Gelosa P and others. 2006. The orphan receptor GPR17 identified as a new dual uracil nucleotides/cysteinyl-leukotrienes receptor. *EMBO J* 25:4615-27.
- Cobelens PM, Kavelaars A, Heijnen CJ, Ribas C, Mayor F, Jr., Penela P. 2007. Hydrogen peroxide impairs GRK2 translation via a calpain-dependent and cdk1-mediated pathway. *Cell Signal* 19:269-77.
- Coppi E, Maraula G, Fumagalli M, Failli P, Cellai L, Bonfanti E, Mazzoni L, Coppini R, Abbracchio MP, Pedata F and others. 2013. UDP-glucose enhances outward K(+) currents necessary for cell differentiation and stimulates cell migration by activating the GPR17 receptor in oligodendrocyte precursors. *Glia* 61:1155-71.
- Daniele S, Trincavelli ML, Fumagalli M, Zappelli E, Lecca D, Bonfanti E, Campiglia P, Abbracchio MP, Martini C. 2014. Does GRK-beta arrestin machinery work as a "switch on" for GPR17-mediated activation of intracellular signaling pathways? *Cell Signal* 26:1310-25.
- Feng J, Tamaskovic R, Yang Z, Brazil DP, Merlo A, Hess D, Hemmings BA. 2004. Stabilization of Mdm2 via decreased ubiquitination is mediated by protein kinase B/Akt-dependent phosphorylation. *J Biol Chem* 279:35510-7.
- Franklin RJ, Ffrench-Constant C. 2008. Remyelination in the CNS: from biology to therapy. *Nat Rev Neurosci* 9:839-55.
- Fratangeli A, Parmigiani E, Fumagalli M, Lecca D, Benfante R, Passafaro M, Buffo A, Abbracchio MP, Rosa P. 2013. The regulated expression, intracellular trafficking and

membrane recycling of the P2Y-like receptor GPR17 in Oli-neu oligodendroglial cells. *J Biol Chem*.

Freedman DA, Wu L, Levine AJ. 1999. Functions of the MDM2 oncoprotein. *Cell Mol Life Sci* 55:96-107.

Fumagalli M, Daniele S, Lecca D, Lee PR, Parravicini C, Fields RD, Rosa P, Antonucci F, Verderio C, Trincavelli ML and others. 2011. Phenotypic changes, signaling pathway, and functional correlates of GPR17-expressing neural precursor cells during oligodendrocyte differentiation. *J Biol Chem* 286:10593-604.

Guardiola-Diaz HM, Ishii A, Bansal R. 2012. Erk1/2 MAPK and mTOR signaling sequentially regulates progression through distinct stages of oligodendrocyte differentiation. *Glia* 60:476-86.

Gurevich EV, Tesmer JJ, Mushegian A, Gurevich VV. 2012. G protein-coupled receptor kinases: more than just kinases and not only for GPCRs. *Pharmacol Ther* 133:40-69.

Hamano K, Iwasaki N, Takeya T, Takita H. 1996. A quantitative analysis of rat central nervous system myelination using the immunohistochemical method for MBP. *Brain Res Dev Brain Res* 93:18-22.

Kuhlmann T, Miron V, Cui Q, Wegner C, Antel J, Bruck W. 2008. Differentiation block of oligodendroglial progenitor cells as a cause for remyelination failure in chronic multiple sclerosis. *Brain* 131:1749-58.

Lecca D, Trincavelli ML, Gelosa P, Sironi L, Ciana P, Fumagalli M, Villa G, Verderio C, Grumelli C, Guerrini U and others. 2008. The recently identified P2Y-like receptor GPR17 is a sensor of brain damage and a new target for brain repair. *PLoS One* 3:e3579.

Lombardi MS, Kavelaars A, Schedlowski M, Bijlsma JW, Okihara KL, Van de Pol M, Ochsmann S, Pawlak C, Schmidt RE, Heijnen CJ. 1999. Decreased expression and activity of G-protein-coupled receptor kinases in peripheral blood mononuclear cells of patients with rheumatoid arthritis. *FASEB J* 13:715-25.

Mayo LD, Donner DB. 2001. A phosphatidylinositol 3-kinase/Akt pathway promotes translocation of Mdm2 from the cytoplasm to the nucleus. *Proc Natl Acad Sci U S A* 98:11598-603.

Narayanan SP, Flores AI, Wang F, Macklin WB. 2009. Akt signals through the mammalian target of rapamycin pathway to regulate CNS myelination. *J Neurosci* 29:6860-70.

Salcedo A, Mayor F, Jr., Penela P. 2006. Mdm2 is involved in the ubiquitination and degradation of G-protein-coupled receptor kinase 2. *EMBO J* 25:4752-62.

Taranto E, Xue JR, Lacey D, Hutchinson P, Smith M, Morand EF, Leech M. 2005. Detection of the p53 regulator murine double-minute protein 2 in rheumatoid arthritis. *J Rheumatol* 32:424-9.

Thut CJ, Goodrich JA, Tjian R. 1997. Repression of p53-mediated transcription by MDM2: a dual mechanism. *Genes Dev* 11:1974-86.

Tyler WA, Gangoli N, Gokina P, Kim HA, Covey M, Levison SW, Wood TL. 2009. Activation of the mammalian target of rapamycin (mTOR) is essential for oligodendrocyte differentiation. *J Neurosci* 29:6367-78.

Tyler WA, Jain MR, Cifelli SE, Li Q, Ku L, Feng Y, Li H, Wood TL. 2011. Proteomic identification of novel targets regulated by the mammalian target of rapamycin pathway during oligodendrocyte differentiation. *Glia* 59:1754-69.

Vassilev LT, Vu BT, Graves B, Carvajal D, Podlaski F, Filipovic Z, Kong N, Kammlott U, Lukacs C, Klein C and others. 2004. In vivo activation of the p53 pathway by small-molecule antagonists of MDM2. *Science* 303:844-8.

Vroon A, Kavelaars A, Limmroth V, Lombardi MS, Goebel MU, Van Dam AM, Caron MG, Schedlowski M, Heijnen CJ. 2005. G protein-coupled receptor kinase 2 in multiple sclerosis and experimental autoimmune encephalomyelitis. *J Immunol* 174:4400-6.

Zappelli E, Daniele S, Abbracchio MP, Martini C, Trincavelli ML. 2014. A rapid and efficient immunoenzymatic assay to detect receptor protein interactions: G protein-coupled receptors. *Int J Mol Sci* 15:6252-64.

Zhao Y, Aguilar A, Bernard D, Wang S. 2015. Small-Molecule Inhibitors of the MDM2-p53 Protein-Protein Interaction (MDM2 Inhibitors) in Clinical Trials for Cancer Treatment. *J Med Chem* 58:1038-52.

## Figure legends

### **Figure 1. mTOR inhibition by rapamycin impairs OPC maturation and increases GPR17 protein levels.**

(A) The scheme shows the experimental protocol of RAPA treatment and the different stages of OPC differentiation, starting from early oligodendrocyte precursors (stage 1) to mature OLs (stage 5). RAPA treatment was started at day 1 and differentiation media with or without RAPA was replenished every 72h. In most cases, analysis was performed at stage 4 and 5 (red circles); the outcome of these experiments is shown in the text. (B) Primary purified OPCs were cultured in the presence of PDGF and of bFGF for two days. Cell differentiation was induced by adding T3 to the medium. RAPA (15 nM) was added at day 1 and day 4. At day 6 (mature OLs, stage 5), cells were fixed for ICC analysis or lysed for WB analysis. Representative images of CTRL and RAPA treated-cells, showing double immunostaining with anti-GPR17 (green) and anti-MBP (red) antibodies. Histograms show the quantification of the percentage of GPR17 and MBP positive cells in control and treated cells (with vehicle-treated control cells set to 100%). Hoechst 33258 was used to label cell nuclei. The number of positive cells was counted in 10 optical fields under a 20X magnification. Data are the mean  $\pm$  S.E. of cell counts from a total of 3 coverslips/condition from three independent experiments,  $**p < 0.01$ ;  $***p < 0.001$  compared to CTRL, Student t-test. (C) Representative immunoblots of GPR17, CNPase and MBP protein levels in CTRL and RAPA treated-cells. Histograms show the results of densitometric analysis. Scanning densitometry was quantified and normalized to control (set to 100%) on the same WB.  $\alpha$ -tubulin expression was analysed from the same samples as an internal control. Data are expressed as mean  $\pm$  S.E. of three independent experiments.  $*p < 0.05$ ;  $**p < 0.01$ ; compared to CTRL, non parametric Mann-Whitney test. (D) Primary OPCs were transfected with a GPR17-EGFP fusion vector for GPR17 over-expression or with the control plasmid (containing EGFP only). After 48/72h, cells were fixed and stained for CNPase

(red). Scale bar 20 $\mu$ m. The percentage of transfected cells expressing CNPase over the total transfected cell population in the two conditions analysed was shown in the histogram. Forced GPR17 over-expression throughout differentiation stages significantly impairs spontaneous cell maturation  $***p < 0.001$  compared to control, Student's t-test, from 4 independent experiments.

**Figure 2. GRK2 plays a key role in mTOR regulation of GPR17 function and OL maturation.** (A) Representative immunoblots of GRK2 protein levels in CTRL and in RAPA treated cells. Histograms show the result of densitometric analysis. Scanning densitometry was quantified and normalized to control (set to 100%) on the same WB.  $\alpha$ -tubulin expression was analysed from the same samples as an internal control. Data from two independent experiments were shown (mean  $\pm$  S.E.,  $*p < 0.05$  compared to CTRL, non parametric Mann-Whitney test). (B) Primary OPCs were treated with medium alone (basal), 5  $\mu$ M UDP-glucose, or 50 nM LTD<sub>4</sub>, in the absence (CTRL) or in the presence of 15 nM RAPA. Cell lysates (30  $\mu$ g) were captured on wells pre-coated with anti-GPR17 antibody. After extensive washes, levels of GPR17/GRK2 complexes were quantified using a specific anti-GRK2 antibody. Data are the mean  $\pm$  S.E. of two independent experiments. One-way ANOVA followed by Bonferroni post-test:  $*p < 0.05$ ,  $***p < 0.001$  vs. basal value. (C) OPCs, isolated and differentiated at pre-oligodendrocytes (stage 3), were treated with 50 nM LTD<sub>4</sub> for different times (5-120 min), in the absence (white bars, CTRL) or in the presence (black bars) of 15 nM RAPA. After extensive washing, cells were treated for 15 min with 10  $\mu$ M FK, in the absence or in the presence of 5 nM LTD<sub>4</sub>. Intracellular cAMP levels were evaluated as reported in Materials and Methods. Data are expressed as the percentage of FK-stimulated cAMP levels, set to 100%, and represent the mean  $\pm$  S.E. of three independent experiments:  $*p < 0.05$ ,  $***p < 0.001$  vs LTD<sub>4</sub> stimuli,  $\#p < 0.05$ ,  $###p < 0.001$  vs relative

control cells, one-way ANOVA followed by Bonferroni post-test. (D) OPCs were electroporated with a GRK2 encoding plasmid. GRK2 over-expression was verified by WB (see the representative immunoblots). 30 h after transfection, cells were treated with 50 nM LTD<sub>4</sub> for different times (30-120 min), in the absence (white bars, CTRL) or presence of 15 nM RAPA (black bars). After extensive washing, cells were treated for 15 min with 10 μM FK, in the absence or in the presence of 5 nM LTD<sub>4</sub> and intracellular cAMP levels were evaluated. Data are expressed as the percentage of FK-stimulated cAMP levels, set to 100%, and represent the mean ± S.E. of two independent experiments. \**p* < 0.05, \*\**p* < 0.01, \*\*\**p* < 0.001 vs LTD<sub>4</sub> stimuli, one-way ANOVA followed by Bonferroni post-test.

**Figure 3. The ubiquitin ligase Mdm2 mediates the interaction between GRK2 and mTOR.** Primary OPCs were pre-incubated for 15 min with 15 nM RAPA (A) or 10 μM NUT (B) and treated with medium alone (basal), or UDP-glucose (5 μM) or with LTD<sub>4</sub> (50 nM), respectively for 30 min. Cell lysates (30 μg) were captured on wells pre-coated with anti-Mdm2 antibody. After extensive washes, levels of Mdm2/GRK complexes were quantified using specific anti-GRK2 or anti-GRK5 antibodies, and subsequently an HRP-conjugated antibody/TMB substrate kit. Blank wells were obtained in the absence of the primary anti-GRK antibodies. Data are expressed as fold vs. basal, and represent the mean ± S.E. of at least three independent experiments. \*\**p* < 0.01; \*\*\**p* < 0.001 vs. basal value, one-way ANOVA with Bonferroni post-test. (C) Primary OPCs (stage 3) were treated with medium alone (CTRL) or 15 nM RAPA for 30 min. At the end of the treatment period, cytosolic and nuclear fractions were collected. Representative immunoblots of Mdm2 levels in CTRL and in RAPA-treated cells. Histograms show the result of densitometric analysis. Scanning densitometry was quantified and normalized to control (set to 100%) on the same WB. α-actin and histone H3 expression were analysed from the same samples as loading controls

for the cytosolic and nuclear fraction, respectively. Data are expressed as mean  $\pm$  S.E. of two independent experiments. One-way ANOVA followed by Bonferroni post-test:  $***p < 0.001$  compared to CTRL. (D) Representative immunoblots of GRK2 and GPR17 and CNPase protein levels in CTRL and in Nutlin-3 (NUT) treated cells. Histograms show the result of densitometric analysis. Scanning densitometry was quantified and normalized to control (set to 100%) on the same WB.  $\alpha$ -tubulin expression was analysed from the same samples as an internal control. Data are expressed as mean  $\pm$  S.E. of two independent experiments,  $*p < 0.05$  compared to CTRL, non parametric Mann-Whitney test. (E) Primary OPCs were treated with medium alone (basal), 5  $\mu$ M UDP-glucose, or 50 nM LTD<sub>4</sub>, in the absence (control) or in the presence of 10  $\mu$ M NUT. Cell lysates (30  $\mu$ g) were captured on wells pre-coated with anti-GPR17 antibody. After extensive washes, levels of GPR17/GRK complexes were quantified using a specific anti-GRK2 antibody. Data are the mean  $\pm$  S.E. of two independent experiments. Statistical significance was determined with a one-way ANOVA with Bonferroni post-test:  $*p < 0.05$ ,  $***p < 0.001$  vs. basal value;  $\#p < 0.05$ ,  $##p < 0.01$ ,  $###p < 0.001$  vs. respective CTRL.

**Figure 4. Sequestration of GRK2 by Mdm2 prevents GPR17 desensitization and OL maturation.** (A) OPCs, isolated and differentiated at pre-oligodendrocytes (stage 3), were treated with 50 nM LTD<sub>4</sub> or 5  $\mu$ M UDP-glucose (B) for different times (5-120 min), in the absence (white bars, CTRL) or presence of 10  $\mu$ M NUT (black bars). After extensive washing, cells were treated for 15 min with 10  $\mu$ M FK, in the absence or in the presence of 500 nM UDP-glucose or 5 nM LTD<sub>4</sub> and intracellular cAMP levels were evaluated. Data are expressed as the percentage of FK-stimulated cAMP levels, set to 100%, and represent the mean  $\pm$  S.E. of three independent experiments.  $*p < 0.05$ ,  $**p < 0.01$ ,  $***p < 0.001$  vs UDP-glucose or LTD<sub>4</sub> stimuli, one-way ANOVA followed by Bonferroni post-test. (C) Primary

purified OPCs were cultured in the presence of PDGF and of bFGF for two days. Cell differentiation was induced by adding T3 to the medium. NUT (1  $\mu$ M) was added at day 1, 30 minutes before treating cells with LTD<sub>4</sub> (100 nM) or with vehicle. The differentiation degree of cells was monitored by analysing the number of cells expressing MBP at stage 4. Representative images of control (CTRL), NUT, LTD<sub>4</sub> and NUT+LTD<sub>4</sub> showing immunostaining with anti-MBP antibody (red). Histograms show the quantification of the percentage of MBP<sup>+</sup> cells in control and treated cells (with vehicle-treated control cells set to 100%). Hoechst 33258 was used to label cell nuclei. The number of MBP<sup>+</sup>-cells was counted in the entire coverslip under a 40X magnification. Data are the mean  $\pm$  S.E. of cell counts from a total of 3 coverslips/condition from three independent experiments \**p* <0.05; \*\**p* <0.01 compared to CTRL, ###*p* <0.01 compared to LTD<sub>4</sub>, non parametric Mann-Whitney test.

**Figure 5. Postnatal in vivo mTOR inhibition with rapamycin alters the normal development of GPR17, GRK2 and myelin associated proteins.** (A) The drawing shows the experimental plan for the in vivo treatment. C57BL6/J mice were injected daily with either vehicle (3 animals) or rapamycin (3 animals) intraperitoneally at a dose of 10 mg/kg body weight, starting from postnatal day (P) 16 to P20. On P21, mice were sacrificed, brains extracted, rapidly frozen at -80°C and processed for western-blot analysis. (B) Representative immunoblots of phospho-mTOR, mTOR, GPR17, GRK2, CNPase and MBP protein levels in control (CTRL) and rapamycin (RAPA) treated mice. Histograms show the result of densitometric analysis. Scanning densitometry was quantified and normalized to control condition (set to 100%) on the same western blot membrane.  $\alpha$ -tubulin expression was analysed from the same samples as an internal control. Data are expressed as mean  $\pm$  S.E. \* *p* <0.05; compared to CTRL, non parametric Mann-Whitney test.

(A) The drawing shows the experimental plan for the in vivo treatment. C57BL6/J mice were injected daily with either vehicle (3 animals) or rapamycin (3 animals) intraperitoneally at a dose of 10 mg/kg body weight, starting from postnatal day (P) 16 to P20. On P21, mice were sacrificed, brains extracted, rapidly frozen at -80°C and processed for western-blot analysis. (B) Representative immunoblots of phospho-mTOR, mTOR, GPR17, GRK2, CNPase and MBP protein levels in control (CTRL) and rapamycin (RAPA) treated mice. Histograms show the result of densitometric analysis. Scanning densitometry was quantified and normalized to control condition (set to 100%) on the same western blot membrane.  $\alpha$ -tubulin expression was analysed from the same samples as an internal control. Data are expressed as mean  $\pm$  S.E. \* *p* <0.05; compared to CTRL, non parametric Mann-Whitney test.

**Figure 6. A cartoon illustrating the signalling pathways involved in GPR17 desensitization/down-regulation and OPC maturation.** (A) Under conditions leading to physiological activation of the mTOR pathway, Mdm2 is mainly associated to the nucleus and bound to p53 and does not interfere with GRK2-mediated GPR17 desensitization in response to LTD<sub>4</sub>. (B) Inhibition of mTOR by rapamycin induced a redistribution of the intracellular concentrations of Mdm2, reducing its nuclear interaction with p53 and increasing the Mdm2/GRK2 association, causing a reduction of the expression levels of GRK2 and a subsequent loss in GPR17 desensitization in response to LTD<sub>4</sub>. The latter event impairs OPC maturation. To confirm the role of Mdm2 in GPR17 desensitization, Nutlin-3, releasing Mdm2 from its complex with p53, favoured the degradation of GRK2 and thus impairing GPR17 desensitization and OPC maturation.

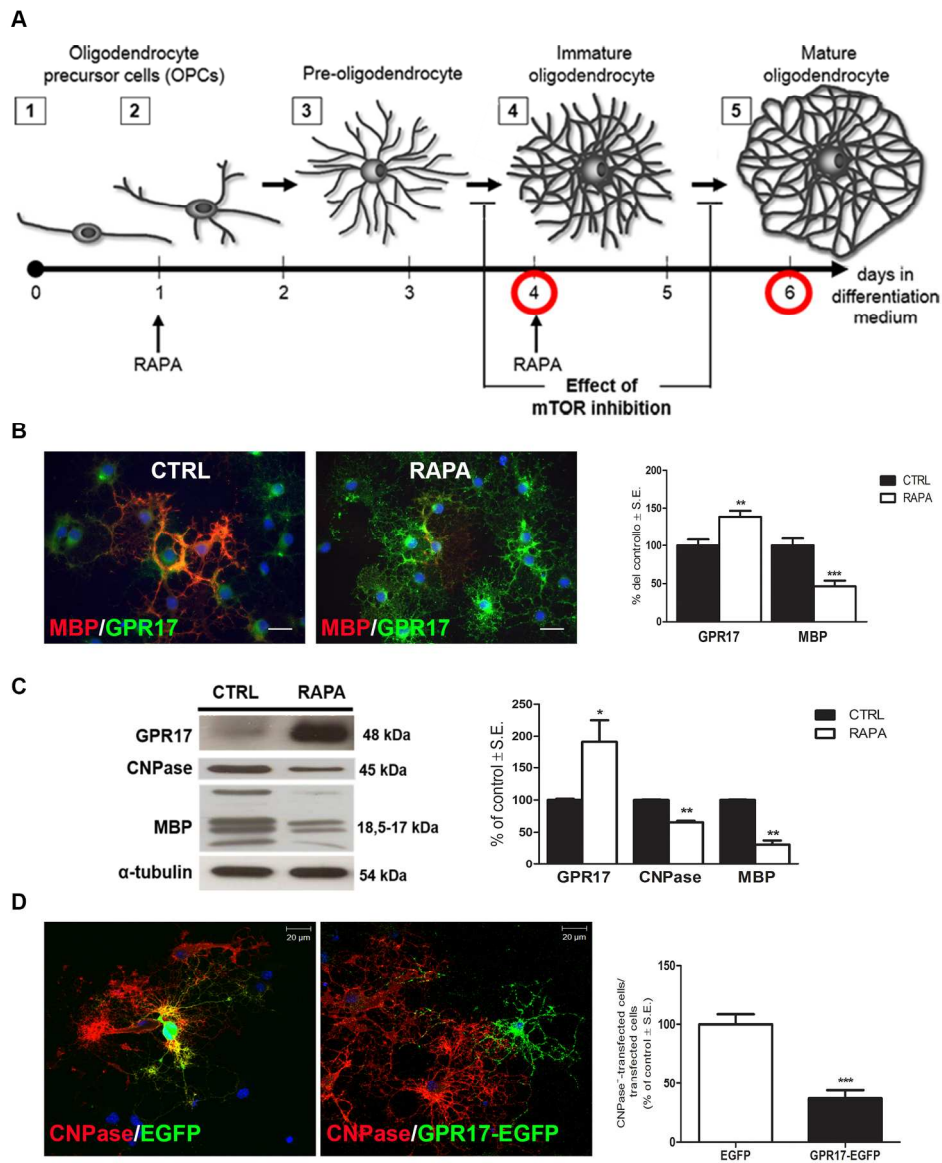


Figure 1. mTOR inhibition by rapamycin impairs OPC maturation and increases GPR17 protein levels. (A) The scheme shows the experimental protocol of RAPA treatment and the different stages of OPC differentiation, starting from early oligodendrocyte precursors (stage 1) to mature OLs (stage 5). RAPA treatment was started at day 1 and differentiation media with or without RAPA was replenished every 72h. In most cases, analysis was performed at stage 4 and 5 (red circles); the outcome of these experiments is shown in the text. (B) Primary purified OPCs were cultured in the presence of PDGF and of bFGF for two days. Cell differentiation was induced by adding T3 to the medium. RAPA (15 nM) was added at day 1 and day 4. At day 6 (mature OLs, stage 5), cells were fixed for ICC analysis or lysed for WB analysis. Representative images of CTRL and RAPA treated-cells, showing double immunostaining with anti-GPR17 (green) and anti-MBP (red) antibodies. Histograms show the quantification of the percentage of GPR17 and MBP positive cells in control and treated cells (with vehicle-treated control cells set to 100%). Hoechst 33258 was used to label cell nuclei. The number of positive cells was counted in 10 optical fields under a 20X magnification. Data are the mean  $\pm$  S.E. of cell counts from a total of 3 coverslips/condition from three independent experiments,

\*\*p <0.01; \*\*\*p <0.001 compared to CTRL, Student t-test. (C) Representative immunoblots of GPR17, CNPase and MBP protein levels in CTRL and RAPA treated-cells. Histograms show the results of densitometric analysis. Scanning densitometry was quantified and normalized to control (set to 100%) on the same WB.  $\alpha$ -tubulin expression was analysed from the same samples as an internal control. Data are expressed as mean  $\pm$  S.E. of three independent experiments. \*p <0.05; \*\*p <0.01; compared to CTRL, non parametric Mann-Whitney test. (D) Primary OPCs were transfected with a GPR17-EGFP fusion vector for GPR17 over-expression or with the control plasmid (containing EGFP only). After 48/72h, cells were fixed and stained for CNPase (red). Scale bar 20 $\mu$ m. The percentage of transfected cells expressing CNPase over the total transfected cell population in the two conditions analysed was shown in the histogram. Forced GPR17 over-expression throughout differentiation stages significantly impairs spontaneous cell maturation \*\*\*p <0.001 compared to control, Student's t-test, from 4 independent experiments.  
181x226mm (300 x 300 DPI)

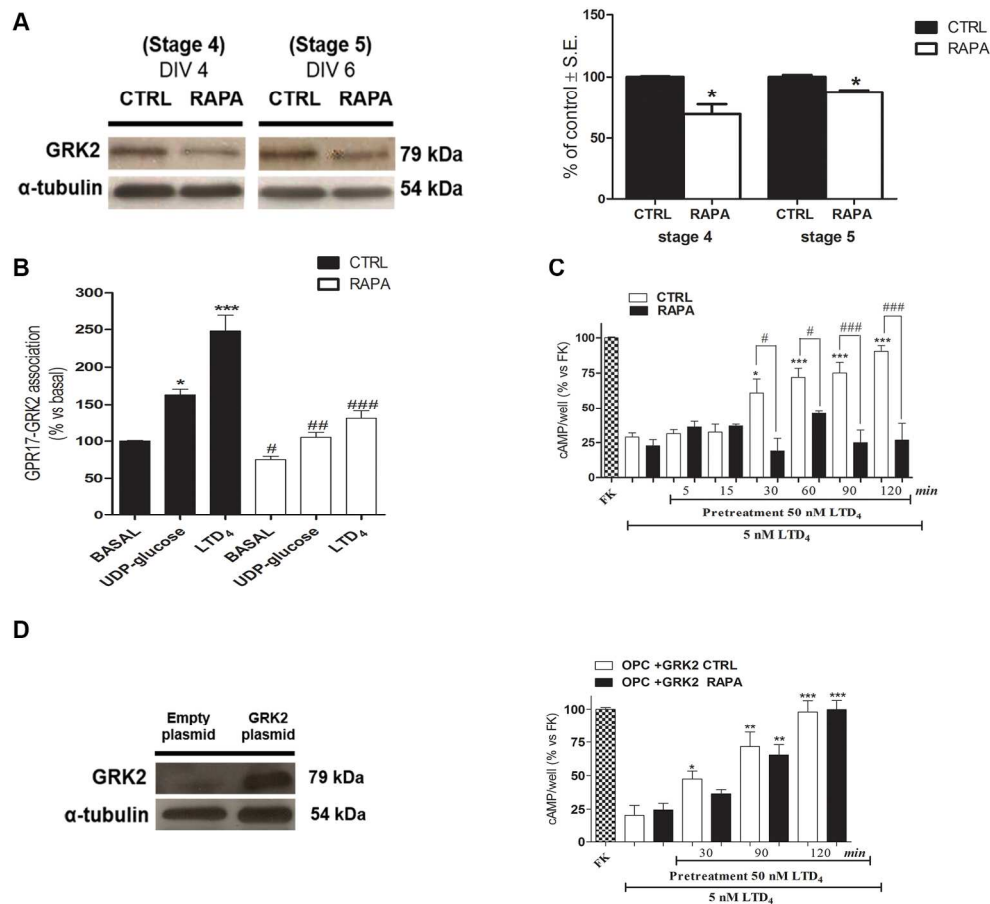


Figure 2. GRK2 plays a key role in mTOR regulation of GPR17 function and OL maturation. (A) Representative immunoblots of GRK2 protein levels in CTRL and in RAPA treated cells. Histograms show the result of densitometric analysis. Scanning densitometry was quantified and normalized to control (set to 100%) on the same WB.  $\alpha$ -tubulin expression was analysed from the same samples as an internal control. Data from two independent experiments were shown (mean  $\pm$  S.E., \* $p$  < 0.05 compared to CTRL, non parametric Mann-Whitney test). (B) Primary OPCs were treated with medium alone (basal), 5  $\mu$ M UDP-glucose, or 50 nM LTD<sub>4</sub>, in the absence (CTRL) or in the presence of 15 nM RAPA. Cell lysates (30  $\mu$ g) were captured on wells pre-coated with anti-GPR17 antibody. After extensive washes, levels of GPR17/GRK2 complexes were quantified using a specific anti-GRK2 antibody. Data are the mean  $\pm$  S.E. of two independent experiments. One-way ANOVA followed by Bonferroni post-test: \* $p$  < 0.05, \*\*\* $p$  < 0.001 vs. basal value. (C) OPCs, isolated and differentiated at pre-oligodendrocytes (stage 3), were treated with 50 nM LTD<sub>4</sub> for different times (5-120 min), in the absence (white bars, CTRL) or in the presence (black bars) of 15 nM RAPA. After extensive washing, cells were treated for 15 min with 10  $\mu$ M FK, in the absence or in the presence of 5 nM LTD<sub>4</sub>. Intracellular cAMP levels were evaluated as reported in Materials and Methods. Data are expressed as the percentage of FK-stimulated cAMP levels, set to 100%, and represent the mean  $\pm$  S.E. of three independent experiments: \* $p$  < 0.05, \*\*\* $p$  < 0.001 vs LTD<sub>4</sub> stimuli, # $p$  < 0.05, ### $p$  < 0.001 vs relative control cells, one-way ANOVA followed by Bonferroni post-test. (D) OPCs were electroporated with a GRK2 encoding plasmid. GRK2 over-expression was verified by WB (see the representative immunoblots). 30 h after transfection, cells were treated with 50 nM LTD<sub>4</sub> for different times (30-120 min), in the absence (white bars, CTRL) or presence of 15 nM RAPA (black bars). After extensive washing, cells were treated for 15 min with 10  $\mu$ M FK, in the absence or in the presence of 5 nM LTD<sub>4</sub> and intracellular cAMP levels were evaluated. Data are expressed as the percentage of FK-stimulated cAMP levels, set to

100%, and represent the mean  $\pm$  S.E. of two independent experiments. \* $p < 0.05$ , \*\* $p < 0.01$ , \*\*\* $p < 0.001$  vs LTD4 stimuli, one-way ANOVA followed by Bonferroni post-test.  
175x167mm (300 x 300 DPI)

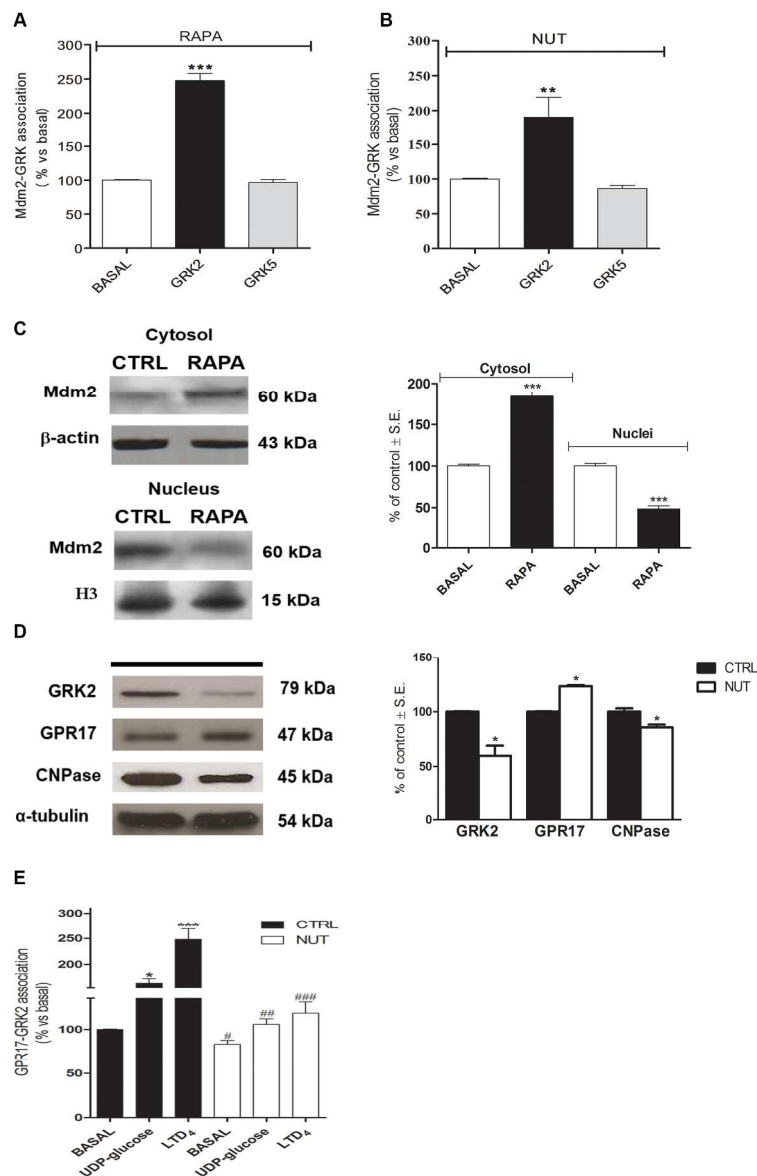


Figure 3. The ubiquitin ligase Mdm2 mediates the interaction between GRK2 and mTOR. Primary OPCs were pre-incubated for 15 min with 15 nM RAPA (A) or 10  $\mu$ M NUT (B) and treated with medium alone (basal), or UDP-glucose (5  $\mu$ M) or with LTD<sub>4</sub> (50 nM), respectively for 30 min. Cell lysates (30  $\mu$ g) were captured on wells pre-coated with anti-Mdm2 antibody. After extensive washes, levels of Mdm2/GRK complexes were quantified using specific anti-GRK2 or anti-GRK5 antibodies, and subsequently an HRP-conjugated antibody/TMB substrate kit. Blank wells were obtained in the absence of the primary anti-GRK antibodies.

Data are expressed as fold vs. basal, and represent the mean  $\pm$  S.E. of at least three independent experiments. \*\* $p$  < 0.01; \*\*\* $p$  < 0.001 vs. basal value, one-way ANOVA with Bonferroni post-test. (C) Primary OPCs (stage 3) were treated with medium alone (CTRL) or 15 nM RAPA for 30 min. At the end of the treatment period, cytosolic and nuclear fractions were collected. Representative immunoblots of Mdm2 levels in CTRL and in RAPA-treated cells. Histograms show the result of densitometric analysis. Scanning densitometry was quantified and normalized to control (set to 100%) on the same WB.  $\alpha$ -actin and histone H3 expression were analysed from the same samples as loading controls for the cytosolic and nuclear

fraction, respectively. Data are expressed as mean  $\pm$  S.E. of two independent experiments. One-way ANOVA followed by Bonferroni post-test: \*\*\* $p < 0.001$  compared to CTRL. (D) Representative immunoblots of GRK2 and GPR17 and CNPase protein levels in CTRL and in Nutlin-3 (NUT) treated cells. Histograms show the result of densitometric analysis. Scanning densitometry was quantified and normalized to control (set to 100%) on the same WB.  $\alpha$ -tubulin expression was analysed from the same samples as an internal control. Data are expressed as mean  $\pm$  S.E. of two independent experiments, \* $p < 0.05$  compared to CTRL, non parametric Mann-Whitney test. (E) Primary OPCs were treated with medium alone (basal), 5  $\mu$ M UDP-glucose, or 50 nM LTD4, in the absence (control) or in the presence of 10  $\mu$ M NUT. Cell lysates (30  $\mu$ g) were captured on wells pre-coated with anti-GPR17 antibody. After extensive washes, levels of GPR17/GRK complexes were quantified using a specific anti-GRK2 antibody. Data are the mean  $\pm$  S.E. of two independent experiments. Statistical significance was determined with a one-way ANOVA with Bonferroni post-test: \* $p < 0.05$ , \*\*\* $p < 0.001$  vs. basal value; # $p < 0.05$ , ## $p < 0.01$ , ### $p < 0.001$  vs. respective CTRL.

175x269mm (300 x 300 DPI)

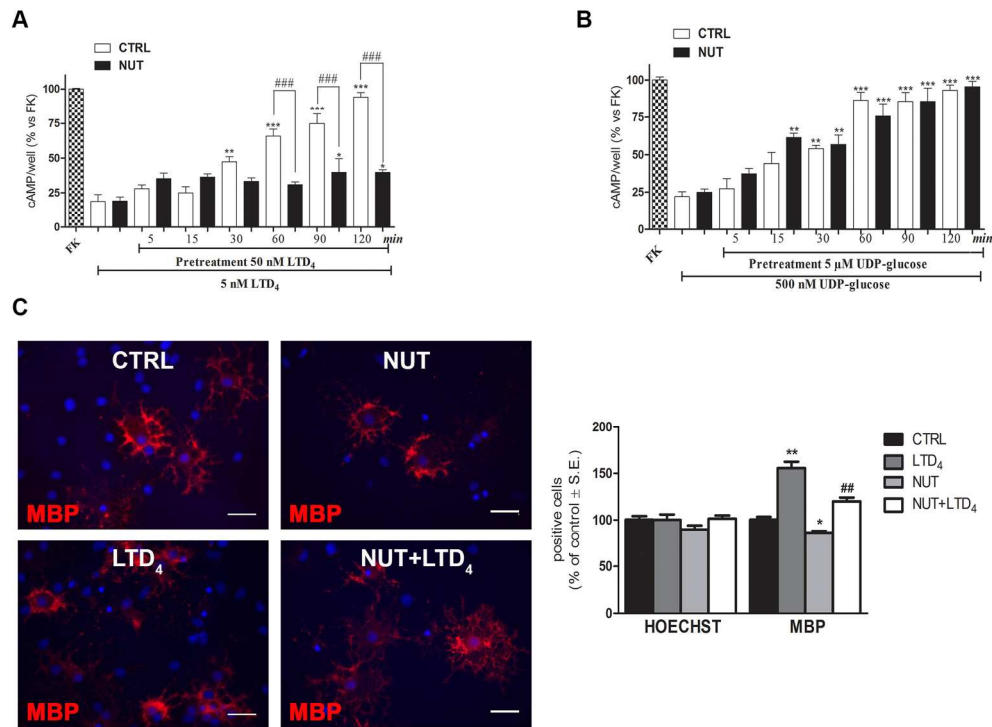


Figure 4. Sequestration of GRK2 by Mdm2 prevents GPR17 desensitization and OL maturation. (A) OPCs, isolated and differentiated at pre-oligodendrocytes (stage 3), were treated with 50 nM LTD<sub>4</sub> or 5 μM UDP-glucose (B) for different times (5-120 min), in the absence (white bars, CTRL) or presence of 10 μM NUT (black bars). After extensive washing, cells were treated for 15 min with 10 μM FK, in the absence or in the presence of 500 nM UDP-glucose or 5 nM LTD<sub>4</sub> and intracellular cAMP levels were evaluated. Data are expressed as the percentage of FK-stimulated cAMP levels, set to 100%, and represent the mean ± S.E. of three independent experiments. \**p* < 0.05, \*\**p* < 0.01, \*\*\**p* < 0.001 vs UDP-glucose or LTD<sub>4</sub> stimuli, one-way ANOVA followed by Bonferroni post-test. (C) Primary purified OPCs were cultured in the presence of PDGF and of bFGF for two days. Cell differentiation was induced by adding T3 to the medium. NUT (1 μM) was added at day 1, 30 minutes before treating cells with LTD<sub>4</sub> (100 nM) or with vehicle. The differentiation degree of cells was monitored by analysing the number of cells expressing MBP at stage 4. Representative images of control (CTRL), NUT, LTD<sub>4</sub> and NUT+LTD<sub>4</sub> showing immunostaining with anti-MBP antibody (red). Histograms show the quantification of the percentage of MBP+ cells in control and treated cells (with vehicle-treated control cells set to 100%). Hoechst 33258 was used to label cell nuclei. The number of MBP+ cells was counted in the entire coverslip under a 40X magnification. Data are the mean ± S.E. of cell counts from a total of 3 coverslips/condition from three independent experiments \**p* < 0.05; \*\**p* < 0.01 compared to CTRL, ##*p* < 0.01 compared to LTD<sub>4</sub>, non parametric Mann-Whitney test. 181x134mm (300 x 300 DPI)

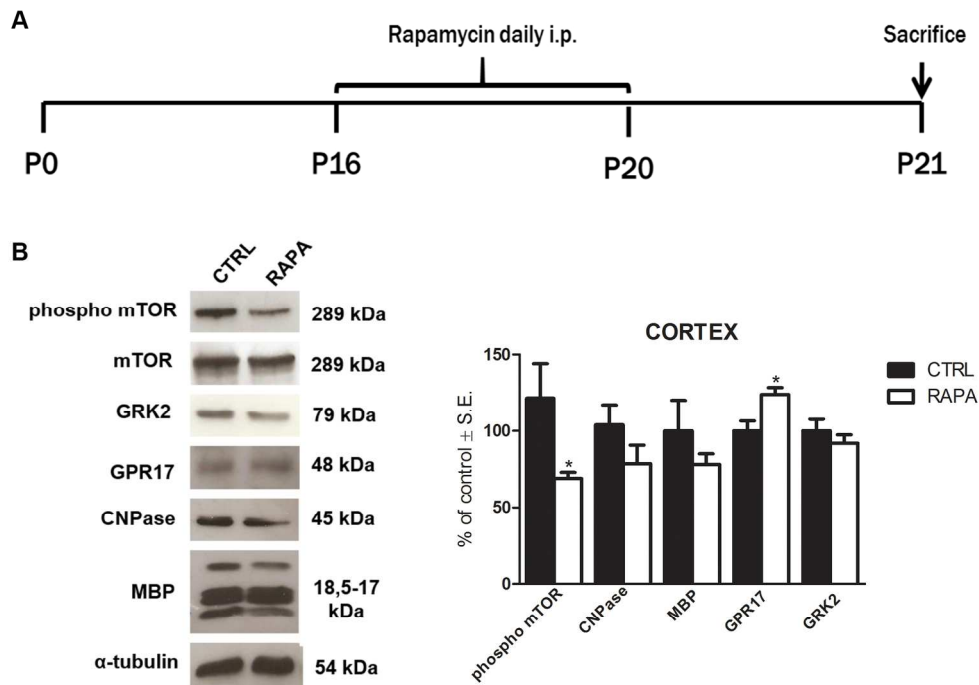


Figure 5. Postnatal in vivo mTOR inhibition with rapamycin alters the normal development of GPR17, GRK2 and myelin associated proteins. (A) The drawing shows the experimental plan for the in vivo treatment. C57BL6/J mice were injected daily with either vehicle (3 animals) or rapamycin (3 animals) intraperitoneally at a dose of 10 mg/kg body weight, starting from postnatal day (P) 16 to P20. On P21, mice were sacrificed, brains extracted, rapidly frozen at  $-80^{\circ}\text{C}$  and processed for western-blot analysis. (B) Representative immunoblots of phospho-mTOR, mTOR, GPR17, GRK2, CNPase and MBP protein levels in control (CTRL) and rapamycin (RAPA) treated mice. Histograms show the result of densitometric analysis. Scanning densitometry was quantified and normalized to control condition (set to 100%) on the same western blot membrane.  $\alpha$ -tubulin expression was analysed from the same samples as an internal control. Data are expressed as mean  $\pm$  S.E. \*  $p < 0.05$ ; compared to CTRL, non parametric Mann-Whitney test.

173x124mm (300 x 300 DPI)

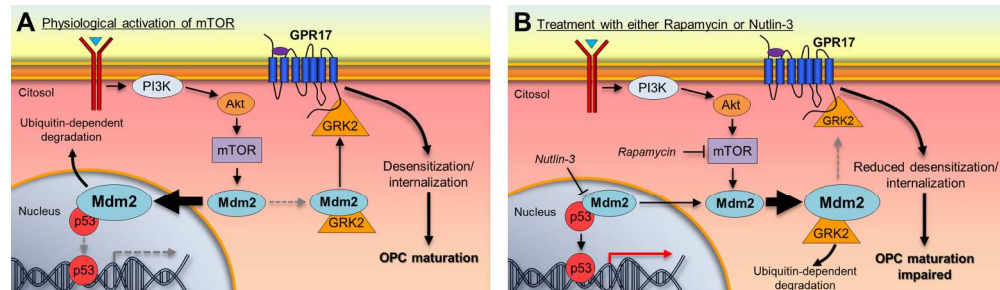


Figure 6. A cartoon illustrating the signalling pathways involved in GPR17 desensitization/down-regulation and OPC maturation. (A) Under conditions leading to physiological activation of the mTOR pathway, Mdm2 is mainly associated to the nucleus and bound to p53 and does not interfere with GRK2-mediated GPR17 desensitization in response to LTD4. (B) Inhibition of mTOR by rapamycin induced a redistribution of the intracellular concentrations of Mdm2, reducing its nuclear interaction with p53 and increasing the Mdm2/GRK2 association, causing a reduction of the expression levels of GRK2 and a subsequent loss in GPR17 desensitization in response to LTD4. The latter event impairs OPC maturation. To confirm the role of Mdm2 in GPR17 desensitization, Nutlin-3, releasing Mdm2 from its complex with p53, favoured the degradation of GRK2 and thus impairing GPR17 desensitization and OPC maturation.

195x55mm (265 x 265 DPI)

**Electronic supplementary material**

**The ubiquitin ligase Mdm2 controls oligodendrocyte maturation by intertwining mTOR with G protein-coupled receptor kinase 2 in the regulation of GPR17 receptor desensitization**

Marta Fumagalli, Elisabetta Bonfanti, Simona Daniele, Elisa Zappelli, Davide Lecca, Claudia Martini, Maria L. Trincavelli, Maria P. Abbraccio

## Supplementary materials and methods

*Myelinating co-cultures.* DRG-OPC co-cultures were prepared according to a previously described protocol (Taveggia et al., 2008). Briefly, DRG from E14.5 mouse embryos were plucked off from spinal cord, put in culture (1 DRG/coverlip) in Neurobasal supplemented with B27 in the presence of NGF (100 ng/ml) (Harlan, Milan, Italy) and cycled with 10  $\mu$ M fluorodeoxyuridine, Sigma Aldrich) to eliminate all non-neuronal cells. After 20 days, when neurites were well extended radially from DRG explants, 35,000 OPCs were added to each DRG in culture and kept in MEM (Life Technologies) supplemented with glucose (4 g/L) (Sigma Aldrich), 10% FBS and 2 mM L-glutamine. Myelination was induced the following day by the addition of recombinant chimeric TrkA-Fc (1  $\mu$ g/ml) (Space Import Export) to the culture medium.

*Co-immunoprecipitation Assay.* Primary OPCs (stage 3) were treated with medium alone (CTRL), 15 nM RAPA or 10  $\mu$ M Nutlin-3 for 30 min, and then lysed for 60 min at 4 °C by the addition of RIPA buffer (9.1 mM NaH<sub>2</sub>PO<sub>4</sub>, 1.7 mM Na<sub>2</sub>HPO<sub>4</sub>, 150 mM NaCl, pH 7.4, 0.5% sodium deoxycholate, 1% Nonidet P-40, and 0.1% SDS, protease inhibitor cocktail). Extracts were then equalised by protein assay. Mdm2 immunoprecipitates were obtained as described previously (Costa et al., 2013). Briefly, 500  $\mu$ g cell lysates were incubated with anti-Mdm2 (Santa Cruz Biotechnology, sc-812; 5  $\mu$ g/sample) overnight at 4 °C under constant rotation. Probes were then immunoprecipitated with protein A-Sepharose (2–3 h at 4 °C). Immunocomplexes, after being washed, were resuspended in Laemmli solution and boiled for 5 min, resolved by SDS-PAGE (8.5%), transferred to PVDF membranes and probed overnight at 4 °C with the specific primary antibodies anti-GRK2 (Santa Cruz Biotechnology, Dallas, TX, USA, sc-562; 1:200) or anti-Mdm2.

~~*In vivo rapamycin injections.* C57BL6/J mice were injected daily with either vehicle or rapamycin intraperitoneally at 10 mg/kg body weight (rapamycin was diluted in the vehicle solution from a stock of 20 mg/mL in 100% ethanol immediately before the injection to a final concentration of 0.8 mg/mL PBS, 5% polyethylene glycol 1000, 5% Tween 80, and 4% ethanol) starting at postnatal day (P) 16. On P21, mice were sacrificed, brains were extracted and rapidly frozen at -80°C. Membrane protein extracts were obtained by tissue homogenization in lysis buffer (20 mM Tris pH 7.2, 0.5% deoxycholate, 1% Triton, 0.1% SDS, 150 mM NaCl, 1 mM EDTA and 1% proteases inhibitors, Sigma Aldrich). The homogenate was centrifuged at 1000g for 10 min at 4°C in order to eliminate nuclei. The protein concentration was estimated using the Bio Rad Protein Assay (Bio Rad Laboratories s.r.l., Segrate, Italy). Western blot analysis was performed as described in the section of Materials and methods.~~

## Supplementary Figure Legends

### **Figure S1. Involvement of mTOR in GPR17 regulation during OPC maturation.** (A)

Primary purified OPCs were cultured in the presence of PDGF and of bFGF for two days. Cell differentiation was induced by adding T3 to the medium. RAPA (15 nM) was added at day 1 and day 4. At day 4 (immature OLs, stage 4), cells were lysed for western-blot analysis. Representative immunoblots of GPR17, CNPase and MBP protein levels in CTRL and RAPA treated-cells. Histograms show the results of densitometric analysis. Scanning densitometry was quantified and normalized to control (set to 100%) on the same WB.  $\alpha$ -tubulin expression was analysed from the same samples as an internal control. Data are expressed as mean  $\pm$  S.E. of three independent experiments. \* $p < 0.05$ ; compared to CTRL, non parametric Mann-Whitney test. (B) OPC/DRG co-cultures were exposed for 10 days to RAPA (15 nM) or vehicle. Representative images of CTRL and RAPA-treated cells show double immunostaining for anti-MBP antibody (red) and anti-neurofilament Smi31 and Smi32 antibodies (indicated as NF, green), scale bar: 20  $\mu$ m.

### **Figure S2. OPCs electroporation with a control vector does not affect GPR17**

**desensitization.** OPCs were transfected by electroporation with the same empty vector utilized for GRK2 transfection (see Fig. 2D). After 30 h, cells were treated with 50 nM LTD4 for different times (30-120 min), in the absence (white bars, CTRL) or presence of 15 nM RAPA (black bars). After extensive washing, cells were treated for 15 min with 10  $\mu$ M FK, in the absence or in the presence of 5 nM LTD4 and intracellular cAMP levels were evaluated. Data are expressed as the percentage of FK-stimulated cAMP levels, set to 100%, and represent the mean  $\pm$  S.E. of two independent experiments. \* $p < 0.05$ , \*\* $p < 0.01$ , \*\*\* $p < 0.001$  vs LTD4 stimuli, one-way ANOVA followed by Bonferroni post-test.

**Figure S3. GRK5 is not involved in mTOR regulation of GPR17 function and OL maturation.** (A) Representative immunoblots of GRK5 protein levels in CTRL and in RAPA treated cells at stage 4 and stage 5. Histograms show the result of densitometric analysis. Scanning densitometry was quantified and normalized to control (set to 100%) on the same WB.  $\alpha$ -tubulin expression was analysed from the same samples as an internal control. Data from two independent experiments were shown. (B) OPCs, isolated and differentiated at pre-oligodendrocytes (stage 3), were treated with 5  $\mu$ M UDP-glucose for different times (5-120 min), in the absence (white bars, CTRL) or in the presence (black bars) of 15 nM RAPA. After extensive washing, cells were treated for 15 min with 10  $\mu$ M FK, in the absence or in the presence of 500 nM UDP-glucose. Intracellular cAMP levels were evaluated as reported in Materials and Methods. Data are expressed as the percentage of FK-stimulated cAMP levels, set to 100%, and represent the mean  $\pm$  S.E. of three independent experiments: \* $P$  < 0.05, \*\* $P$  < 0.01, \*\*\* $P$  < 0.001 vs UDP-glucose stimuli, one-way ANOVA followed by Bonferroni post-test

~~**Figure S3 Postnatal *in vivo* mTOR inhibition with rapamycin alters the normal development of GPR17, GRK2 and myelin associated proteins.**~~ (A) The drawing shows the experimental plan for the *in vivo* treatment. C57BL6/J mice were injected daily with either vehicle (3 animals) or rapamycin (3 animals) intraperitoneally at a dose of 10 mg/kg body weight, starting from postnatal day (P) 16 to P20. On P21, mice were sacrificed, brains extracted, rapidly frozen at  $-80^{\circ}\text{C}$  and processed for western blot analysis. (B) Representative immunoblots of phospho-mTOR, mTOR, GPR17, GRK2, CNPase and MBP protein levels in control (CTRL) and rapamycin (RAPA) treated mice. Histograms show the result of densitometric analysis. Scanning densitometry was quantified and normalized to control

~~condition (set to 100%) on the same western blot membrane.  $\alpha$  tubulin expression was analysed from the same samples as an internal control.~~

**Figure S4. Both RAPA and NUT markedly reduce the Mdm2-p53 association complex.**

Primary OPCs (stage 3) were treated with either medium alone (basal), or 15 nM RAPA or 10  $\mu$ M Nutlin-3 for 30 min. At the end of treatments, OPCs were lysed and then captured on wells pre-coated with anti-Mdm2 antibody. After extensive washes, levels of Mdm2/p53 complexes were quantified using a specific anti-p53 antibody. Data are the mean  $\pm$  S.E. of two independent experiments. One-way ANOVA followed by Bonferroni post-test: \*\* $p < 0.001$ , \*\*\* $p < 0.001$  vs. basal value.

**Figure S5. Both RAPA and NUT increase the interaction between Mdm2 and GRK2.**

Primary OPCs (stage 3) were treated with either medium alone (CTRL), or 15 nM RAPA or 10  $\mu$ M Nutlin-3 for 30 min. (A) Representative immunoblots of Mdm2-GRK2 immunocomplex levels in CTRL, RAPA and in NUT treated cells. Histograms show the result of densitometric analysis. Scanning densitometry was quantified and normalized to control (set to 100%) on the same WB. Mdm2 expression was analysed from the same samples as internal control. Data are expressed as mean  $\pm$  S.E. of two independent experiments. One-way ANOVA followed by Bonferroni post-test: \*\* $p < 0.01$ , \*\*\* $p < 0.001$  compared to CTRL.

**Supplementary References**

Taveggia C, Thaker P, Petrylak A, Caporaso GL, Toews A, Falls DL, Einheber S, Salzer JL. 2008. Type III neuregulin-1 promotes oligodendrocyte myelination. *Glia* 56:284-93.

Costa B, Bendinelli S, Gabelloni P, Da Pozzo E, Daniele S, Scatena F, Vanacore R, Campiglia P, Bertamino A, Gomez-Monterrey I, Sorriente D, Del Giudice C, Iaccarino G, Novellino E, Martini C. Human glioblastoma multiforme: p53 reactivation by a novel MDM2 inhibitor. *Plos One* 8:e72281.

**Electronic supplementary material**

**The ubiquitin ligase Mdm2 controls oligodendrocyte maturation by intertwining mTOR with G protein-coupled receptor kinase 2 in the regulation of GPR17 receptor desensitization**

Marta Fumagalli, Elisabetta Bonfanti, Simona Daniele, Elisa Zappelli, Davide Lecca, Claudia Martini, Maria L. Trincavelli, Maria P. Abbracchio

## Supplementary materials and methods

*Myelinating co-cultures.* DRG-OPC co-cultures were prepared according to a previously described protocol (Taveggia et al., 2008). Briefly, DRG from E14.5 mouse embryos were plucked off from spinal cord, put in culture (1 DRG/coverlip) in Neurobasal supplemented with B27 in the presence of NGF (100 ng/ml) (Harlan, Milan, Italy) and cycled with 10  $\mu$ M fluorodeoxyuridine, Sigma Aldrich) to eliminate all non-neuronal cells. After 20 days, when neurites were well extended radially from DRG explants, 35,000 OPCs were added to each DRG in culture and kept in MEM (Life Technologies) supplemented with glucose (4 g/L) (Sigma Aldrich), 10% FBS and 2 mM L-glutamine. Myelination was induced the following day by the addition of recombinant chimeric TrkA-Fc (1  $\mu$ g/ml) (Space Import Export) to the culture medium.

*Co-immunoprecipitation Assay.* Primary OPCs (stage 3) were treated with medium alone (CTRL), 15 nM RAPA or 10  $\mu$ M Nutlin-3 for 30 min, and then lysed for 60 min at 4 °C by the addition of RIPA buffer (9.1 mM NaH<sub>2</sub>PO<sub>4</sub>, 1.7 mM Na<sub>2</sub>HPO<sub>4</sub>, 150 mM NaCl, pH 7.4, 0.5% sodium deoxycholate, 1% Nonidet P-40, and 0.1% SDS, protease inhibitor cocktail). Extracts were then equalised by protein assay. Mdm2 immunoprecipitates were obtained as described previously (Costa et al., 2013). Briefly, 500  $\mu$ g cell lysates were incubated with anti-Mdm2 (Santa Cruz Biotechnology, sc-812; 5  $\mu$ g/sample) overnight at 4 °C under constant rotation. Probes were then immunoprecipitated with protein A-Sepharose (2–3 h at 4 °C). Immunocomplexes, after being washed, were resuspended in Laemmli solution and boiled for 5 min, resolved by SDS-PAGE (8.5%), transferred to PVDF membranes and probed overnight at 4 °C with the specific primary antibodies anti-GRK2 (Santa Cruz Biotechnology, Dallas, TX, USA, sc-562; 1:200) or anti-Mdm2.

## Supplementary Figure Legends

### **Figure S1. Involvement of mTOR in GPR17 regulation during OPC maturation.** (A)

Primary purified OPCs were cultured in the presence of PDGF and of bFGF for two days. Cell differentiation was induced by adding T3 to the medium. RAPA (15 nM) was added at day 1 and day 4. At day 4 (immature OLs, stage 4), cells were lysed for western-blot analysis. Representative immunoblots of GPR17, CNPase and MBP protein levels in CTRL and RAPA treated-cells. Histograms show the results of densitometric analysis. Scanning densitometry was quantified and normalized to control (set to 100%) on the same WB.  $\alpha$ -tubulin expression was analysed from the same samples as an internal control. Data are expressed as mean  $\pm$  S.E. of three independent experiments. \* $p < 0.05$ ; compared to CTRL, non parametric Mann-Whitney test. (B) OPC/DRG co-cultures were exposed for 10 days to RAPA (15 nM) or vehicle. Representative images of CTRL and RAPA-treated cells show double immunostaining for anti-MBP antibody (red) and anti-neurofilament Smi31 and Smi32 antibodies (indicated as NF, green), scale bar: 20  $\mu$ m.

### **Figure S2. OPCs electroporation with a control vector does not affect GPR17**

**desensitization.** OPCs were transfected by electroporation with the same empty vector utilized for GRK2 transfection (see Fig. 2D). After 30 h, cells were treated with 50 nM LTD4 for different times (30-120 min), in the absence (white bars, CTRL) or presence of 15 nM RAPA (black bars). After extensive washing, cells were treated for 15 min with 10  $\mu$ M FK, in the absence or in the presence of 5 nM LTD4 and intracellular cAMP levels were evaluated. Data are expressed as the percentage of FK-stimulated cAMP levels, set to 100%, and represent the mean  $\pm$  S.E. of two independent experiments. \* $p < 0.05$ , \*\* $p < 0.01$ , \*\*\* $p < 0.001$  vs LTD4 stimuli, one-way ANOVA followed by Bonferroni post-test.

**Figure S3. GRK5 is not involved in mTOR regulation of GPR17 function and OL maturation.** (A) Representative immunoblots of GRK5 protein levels in CTRL and in RAPA treated cells at stage 4 and stage 5. Histograms show the result of densitometric analysis. Scanning densitometry was quantified and normalized to control (set to 100%) on the same WB.  $\alpha$ -tubulin expression was analysed from the same samples as an internal control. Data from two independent experiments were shown. (B) OPCs, isolated and differentiated at pre-oligodendrocytes (stage 3), were treated with 5  $\mu$ M UDP-glucose for different times (5-120 min), in the absence (white bars, CTRL) or in the presence (black bars) of 15 nM RAPA. After extensive washing, cells were treated for 15 min with 10  $\mu$ M FK, in the absence or in the presence of 500 nM UDP-glucose. Intracellular cAMP levels were evaluated as reported in Materials and Methods. Data are expressed as the percentage of FK-stimulated cAMP levels, set to 100%, and represent the mean  $\pm$  S.E. of three independent experiments: \* $P$  <0.05, \*\* $P$ <0.01, \*\*\* $P$ <0.001 vs UDP-glucose stimuli, one-way ANOVA followed by Bonferroni post-test

**Figure S4. Both RAPA and NUT markedly reduce the Mdm2-p53 association complex.** Primary OPCs (stage 3) were treated with either medium alone (basal), or 15 nM RAPA or 10  $\mu$ M Nutlin-3 for 30 min. At the end of treatments, OPCs were lysed and then captured on wells pre-coated with anti-Mdm2 antibody. After extensive washes, levels of Mdm2/p53 complexes were quantified using a specific anti-p53 antibody. Data are the mean  $\pm$  S.E. of two independent experiments. One-way ANOVA followed by Bonferroni post-test: \*\* $p$  <0.001, \*\*\* $p$  <0.001 vs. basal value.

**Figure S5. Both RAPA and NUT increase the interaction between Mdm2 and GRK2.** Primary OPCs (stage 3) were treated with either medium alone (CTRL), or 15 nM RAPA or

10  $\mu$ M Nutlin-3 for 30 min. (A) Representative immunoblots of Mdm2-GRK2 immunocomplex levels in CTRL, RAPA and in NUT treated cells. Histograms show the result of densitometric analysis. Scanning densitometry was quantified and normalized to control (set to 100%) on the same WB. Mdm2 expression was analysed from the same samples as internal control. Data are expressed as mean  $\pm$  S.E. of two independent experiments. One-way ANOVA followed by Bonferroni post-test:  $**p < 0.01$ ,  $***p < 0.001$  compared to CTRL.

**Supplementary References**

Taveggia C, Thaker P, Petrylak A, Caporaso GL, Toews A, Falls DL, Einheber S, Salzer JL. 2008. Type III neuregulin-1 promotes oligodendrocyte myelination. *Glia* 56:284-93.

Costa B, Bendinelli S, Gabelloni P, Da Pozzo E, Daniele S, Scatena F, Vanacore R, Campiglia P, Bertamino A, Gomez-Monterrey I, Sorriente D, Del Giudice C, Iaccarino G, Novellino E, Martini C. Human glioblastoma multiforme: p53 reactivation by a novel MDM2 inhibitor. *Plos One* 8:e72281.

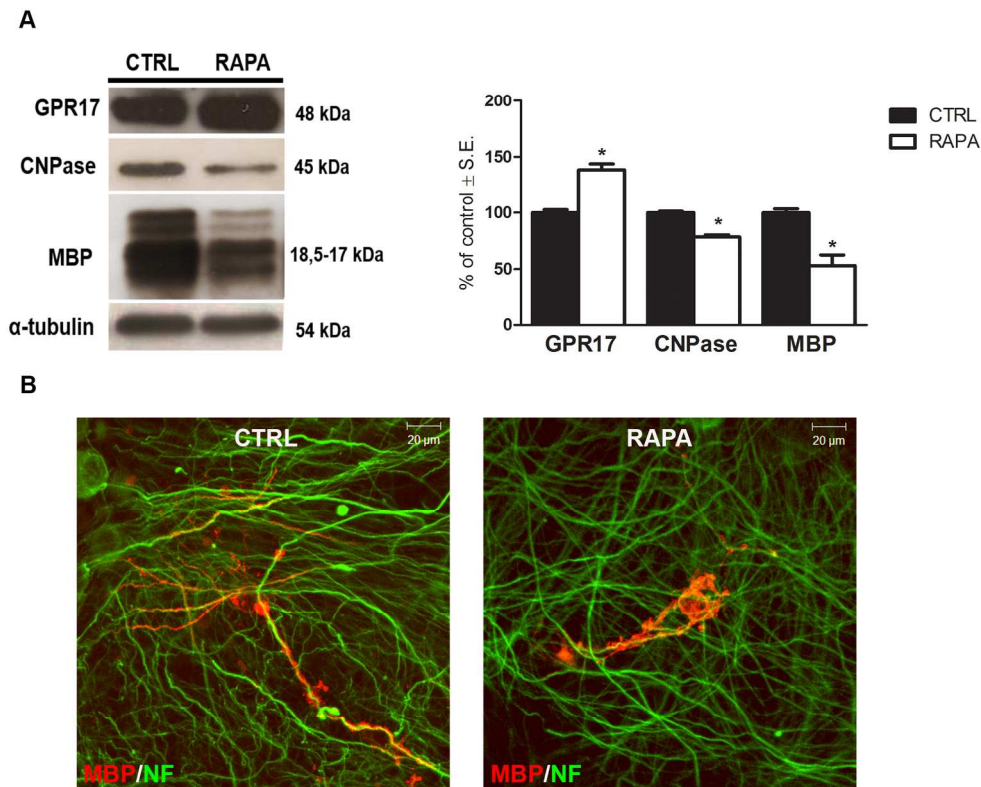


Figure S1. Involvement of mTOR in GPR17 regulation during OPC maturation. (A) Primary purified OPCs were cultured in the presence of PDGF and of bFGF for two days. Cell differentiation was induced by adding T3 to the medium. RAPA (15 nM) was added at day 1 and day 4. At day 4 (immature OLs, stage 4), cells were lysed for western-blot analysis. Representative immunoblots of GPR17, CNPase and MBP protein levels in CTRL and RAPA treated-cells. Histograms show the results of densitometric analysis. Scanning densitometry was quantified and normalized to control (set to 100%) on the same WB.  $\alpha$ -tubulin expression was analysed from the same samples as an internal control. Data are expressed as mean  $\pm$  S.E. of three independent experiments. \* $p < 0.05$ ; compared to CTRL, non parametric Mann-Whitney test. (B) OPC/DRG co-cultures were exposed for 10 days to RAPA (15 nM) or vehicle. Representative images of CTRL and RAPA-treated cells show double immunostaining for anti-MBP antibody (red) and anti-neurofilament Smi31 and Smi32 antibodies (indicated as NF, green), scale bar: 20  $\mu$ m.

177x146mm (300 x 300 DPI)

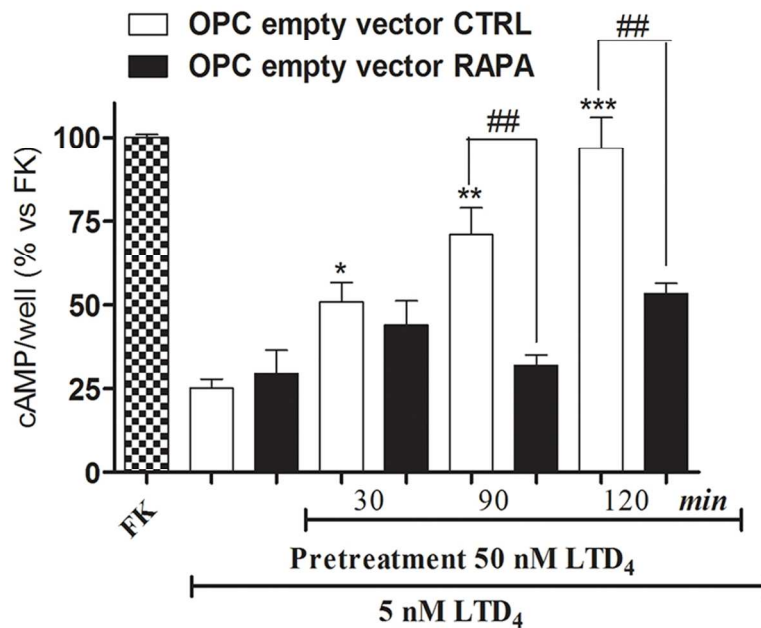


Figure S2. OPCs electroporation with a control vector does not affect GPR17 desensitization. OPCs were transfected by electroporation with the same empty vector utilized for GRK2 transfection (see Fig. 2D). After 30 h, cells were treated with 50 nM LTD<sub>4</sub> for different times (30-120 min), in the absence (white bars, CTRL) or presence of 15 nM RAPA (black bars). After extensive washing, cells were treated for 15 min with 10  $\mu$ M FK, in the absence or in the presence of 5 nM LTD<sub>4</sub> and intracellular cAMP levels were evaluated. Data are expressed as the percentage of FK-stimulated cAMP levels, set to 100%, and represent the mean  $\pm$  S.E. of two independent experiments. \* $p$  < 0.05, \*\* $p$  < 0.01, \*\*\* $p$  < 0.001 vs LTD<sub>4</sub> stimuli, one-way ANOVA followed by Bonferroni post-test.

86x65mm (300 x 300 DPI)

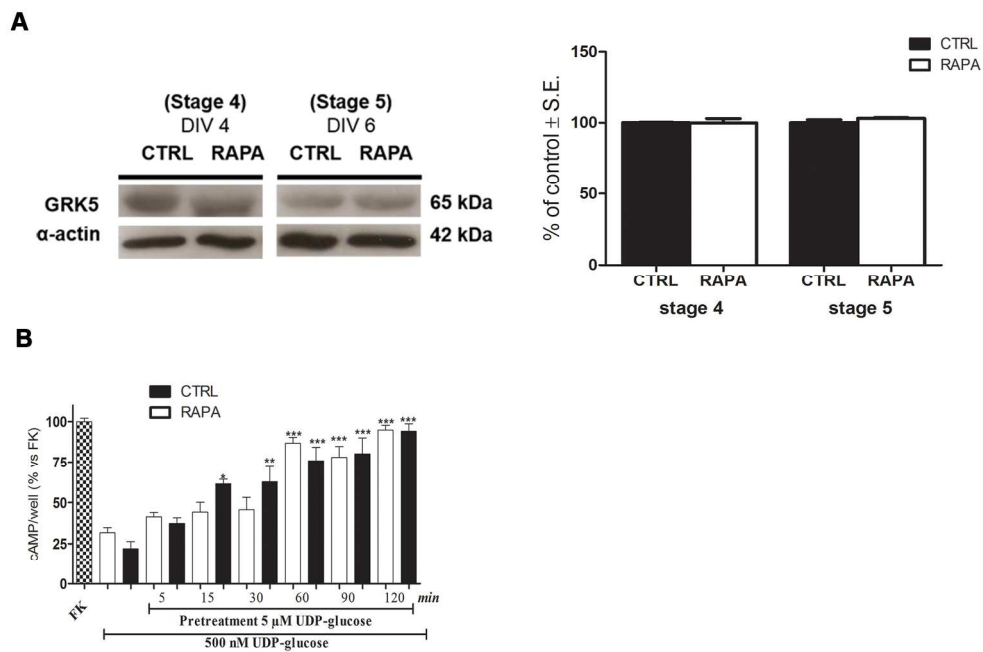


Figure S3. GRK5 is not involved in mTOR regulation of GPR17 function and OL maturation. (A) Representative immunoblots of GRK5 protein levels in CTRL and in RAPA treated cells at stage 4 and stage 5. Histograms show the result of densitometric analysis. Scanning densitometry was quantified and normalized to control (set to 100%) on the same WB.  $\alpha$ -tubulin expression was analysed from the same samples as an internal control. Data from two independent experiments were shown. (B) OPCs, isolated and differentiated at pre-oligodendrocytes (stage 3), were treated with 5  $\mu$ M UDP-glucose for different times (5-120 min), in the absence (white bars, CTRL) or in the presence (black bars) of 15 nM RAPA. After extensive washing, cells were treated for 15 min with 10  $\mu$ M FK, in the absence or in the presence of 500 nM UDP-glucose. Intracellular cAMP levels were evaluated as reported in Materials and Methods. Data are expressed as the percentage of FK-stimulated cAMP levels, set to 100%, and represent the mean  $\pm$  S.E. of three independent experiments: \*P < 0.05, \*\*P < 0.01, \*\*\*P < 0.001 vs UDP-glucose stimuli, one-way ANOVA followed by Bonferroni post-test.  
175x115mm (300 x 300 DPI)

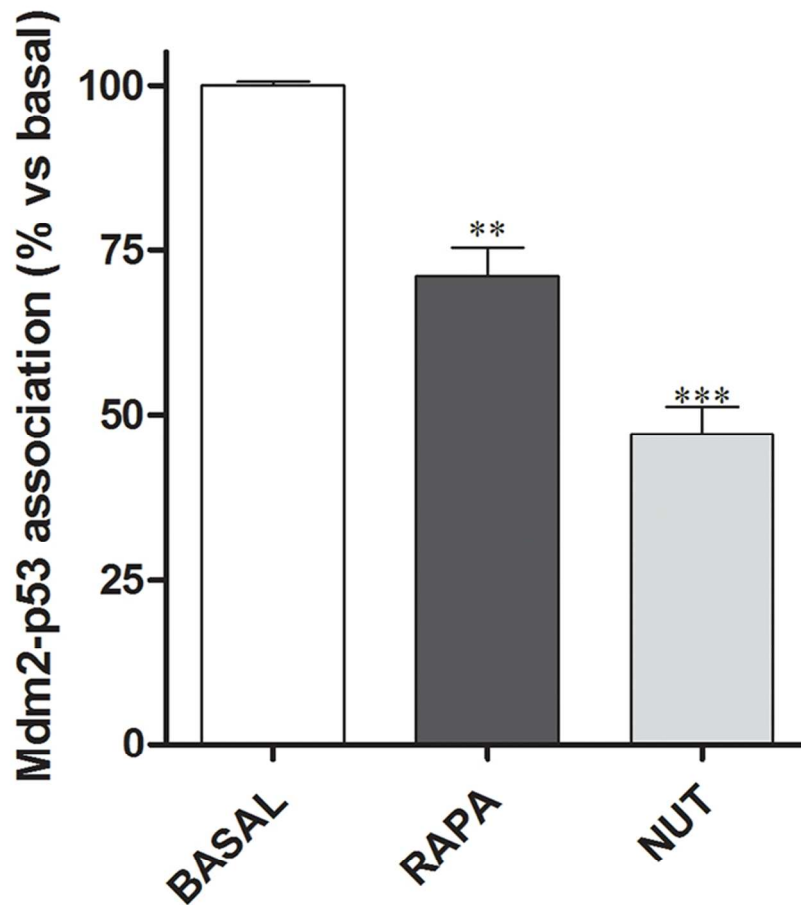


Figure S4. Both RAPA and NUT markedly reduce the Mmd2-p53 association complex. Primary OPCs (stage 3) were treated with either medium alone (basal), or 15 nM RAPA or 10  $\mu$ M Nutlin-3 for 30 min. At the end of treatments, OPCs were lysed and then captured on wells pre-coated with anti-Mdm2 antibody. After extensive washes, levels of Mdm2/p53 complexes were quantified using a specific anti-p53 antibody. Data are the mean  $\pm$  S.E. of two independent experiments. One-way ANOVA followed by Bonferroni post-test:

\*\*p <0.001, \*\*\*p <0.001 vs. basal value.

73x78mm (300 x 300 DPI)

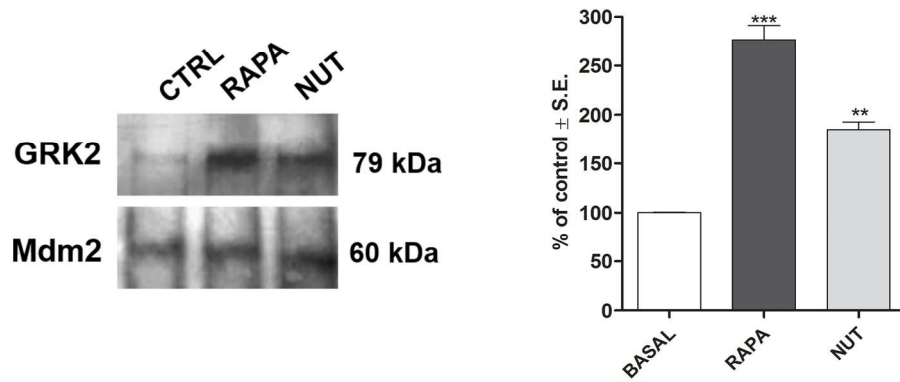


Figure S5. Both RAPA and NUT increase the interaction between Mdm2 and GRK2. Primary OPCs (stage 3) were treated with either medium alone (CTRL), or 15 nM RAPA or 10  $\mu$ M Nutlin-3 for 30 min. (A) Representative immunoblots of Mdm2-GRK2 immunocomplex levels in CTRL, RAPA and in NUT treated cells. Histograms show the result of densitometric analysis. Scanning densitometry was quantified and normalized to control (set to 100%) on the same WB. Mdm2 expression was analysed from the same samples as internal control. Data are expressed as mean  $\pm$  S.E. of two independent experiments. One-way ANOVA followed by Bonferroni post-test: \*\* $p < 0.01$ , \*\*\* $p < 0.001$  compared to CTRL.  
176x80mm (300 x 300 DPI)